Genetic Toxicology & DNA Repair Research at Stony Brook: Department of Pharmacological Sciences

Carlos de los Santos: **TODAY'S SPEAKER**

***Dan Bogenhagen*: DNA replication and repair in mitochondria**

***Bruce Demple**: Oxidative DNA damage; BER; oxidative stress responses**

***Miguel Garcia-Diaz**: DNA replication fidelity; protein structure; gene regulation in mitochondria**

***Arthur Grollman*: Mutagenesis and molecular carcinogenesis (aristolochic acid); structural biology**

***Francis Johnson & Charles Iden*: Synthesis, purification and analysis of single-lesion DNA molecules**

***Orlando Schärer*: Mechanisms of mammalian NER; DNA interstrand crosslinks**

***Kate Dickman*: DNA damage and renal disease**

***Mark Lukin*: generation of site-specific DNA lesions**

***Masaaki Moriya*: translesion DNA polymerases**

***Mamta Naidu*: Radiation biology & BER; heavy ion studies**

***Thomas Rosenquist*: genetics of aristolochic acid toxicology**

***Recruited through Consortium for InterDisciplinary Environmental Research**

STONY BROOK
STATE UNIVERSITY OF NEW YORK

New insights into NER recognition: When bulky & perturbing is not enough

4/17/12

Kwong-Ngai Hung
Serge Smirnov
David Cullinam
Zhen Lin
Jenifer Bohon
Raphael Hazel
Omar Armstrong
Tanya Zaliznyak
Smita Mohanty
Mahmoud El-Katheeb
Kegui Tian
Freda Sansaricq
Dmitry Zamyatkin
Kimberly Conlon
Monica McTigue

Arthur Grollman
Francis Johnson
Charles Iden
Carlos Simmerling
Orlando Scharer
Miguel Garcia-Diaz
Masaaki Moriya
Mark Lukin

NCI, NIEHS

Healthy Genome

DNA Damage Rate < Repair Rate

Sick Cell

DNA Damage Rate > Repair Rate

Cancer

Ageing

Repair Diseases

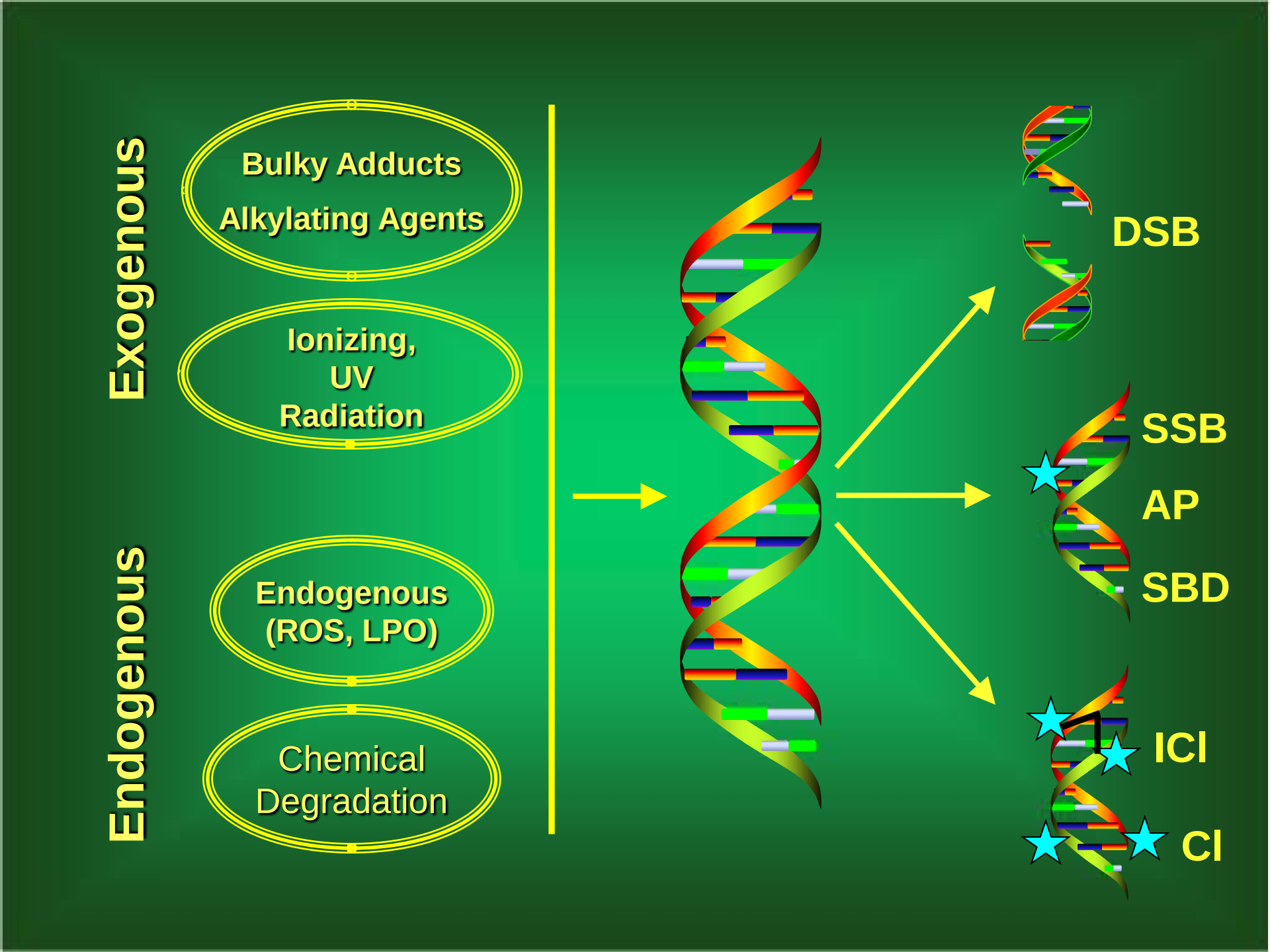
Exogenous
Bulky Adducts
Alkylating Agents
Ionizing,
UV
Radiation
Endogenous
Endogenous
(ROS, LPO)
Chemical
Degradation
DSB
SSB
AP
SBD
ICl
Cl

DNA Damage and Repair

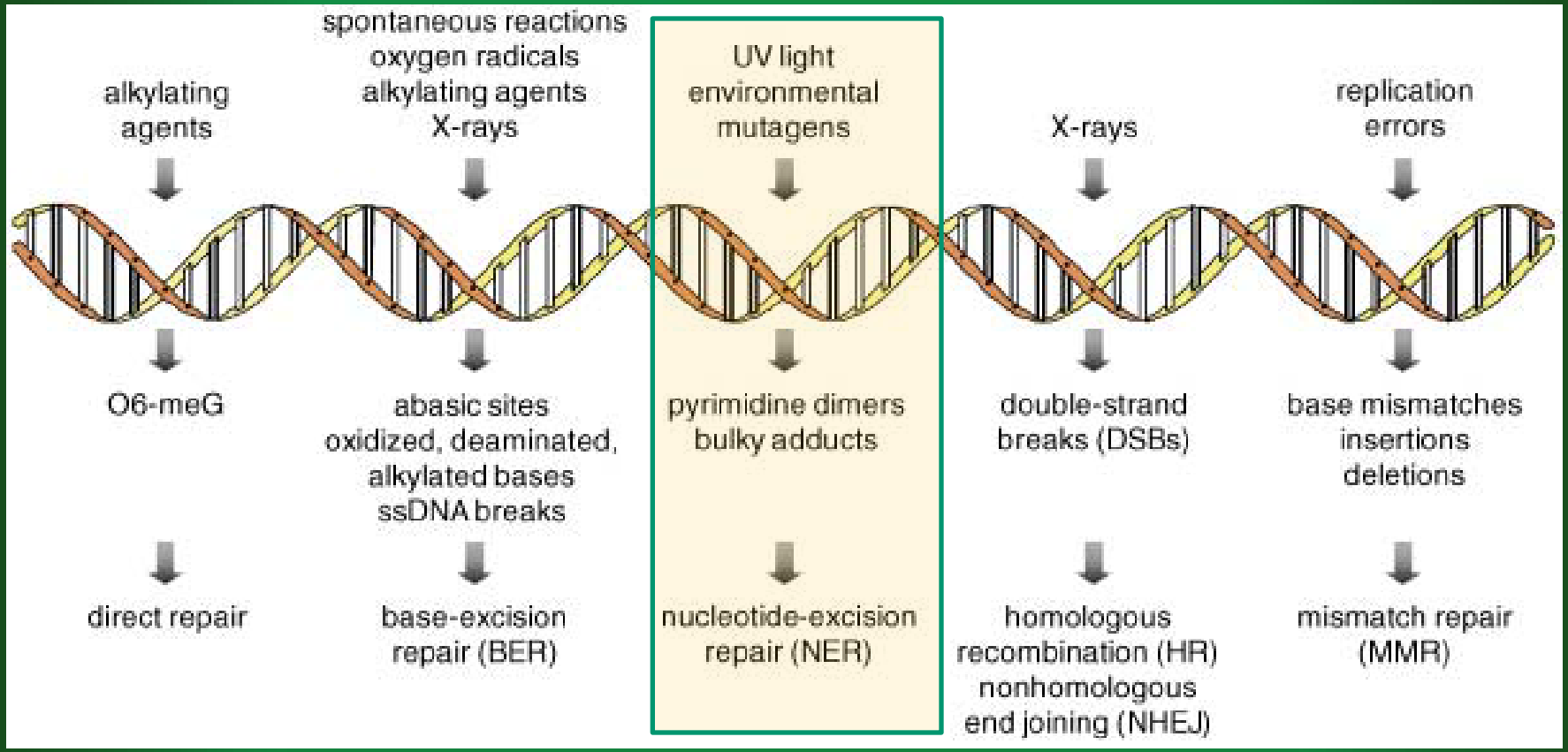

NER Lesions

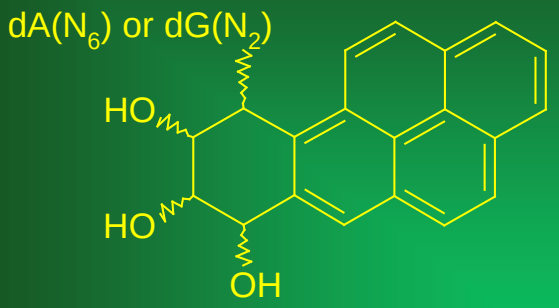

Benzo[a]Pyrene

2-Nitrofluorene

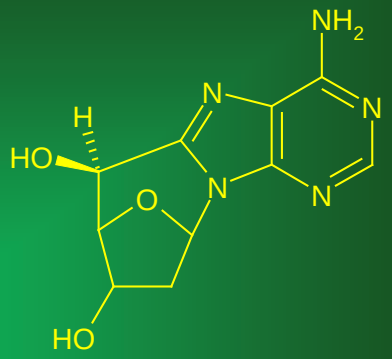

5',8-cyclo-dA

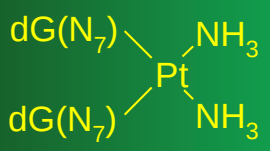

cis-platinum

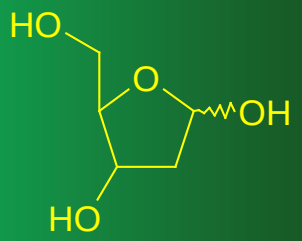

AP Sites

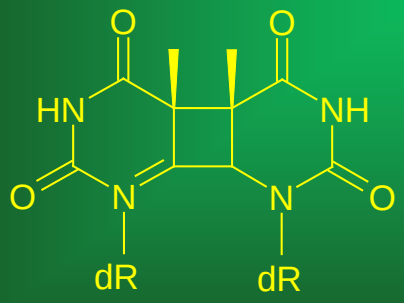

Cyclobutane TT dimer

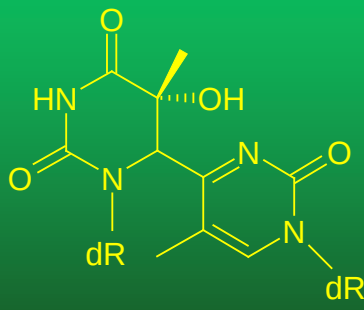

6-4 Photoproducts

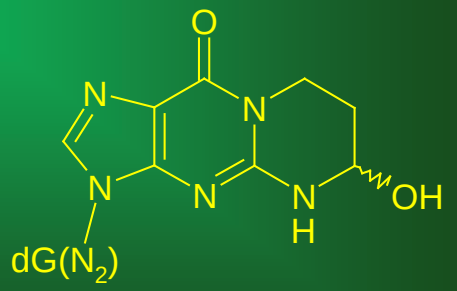

Acrolein

NER Recognition of Bulky Adducts

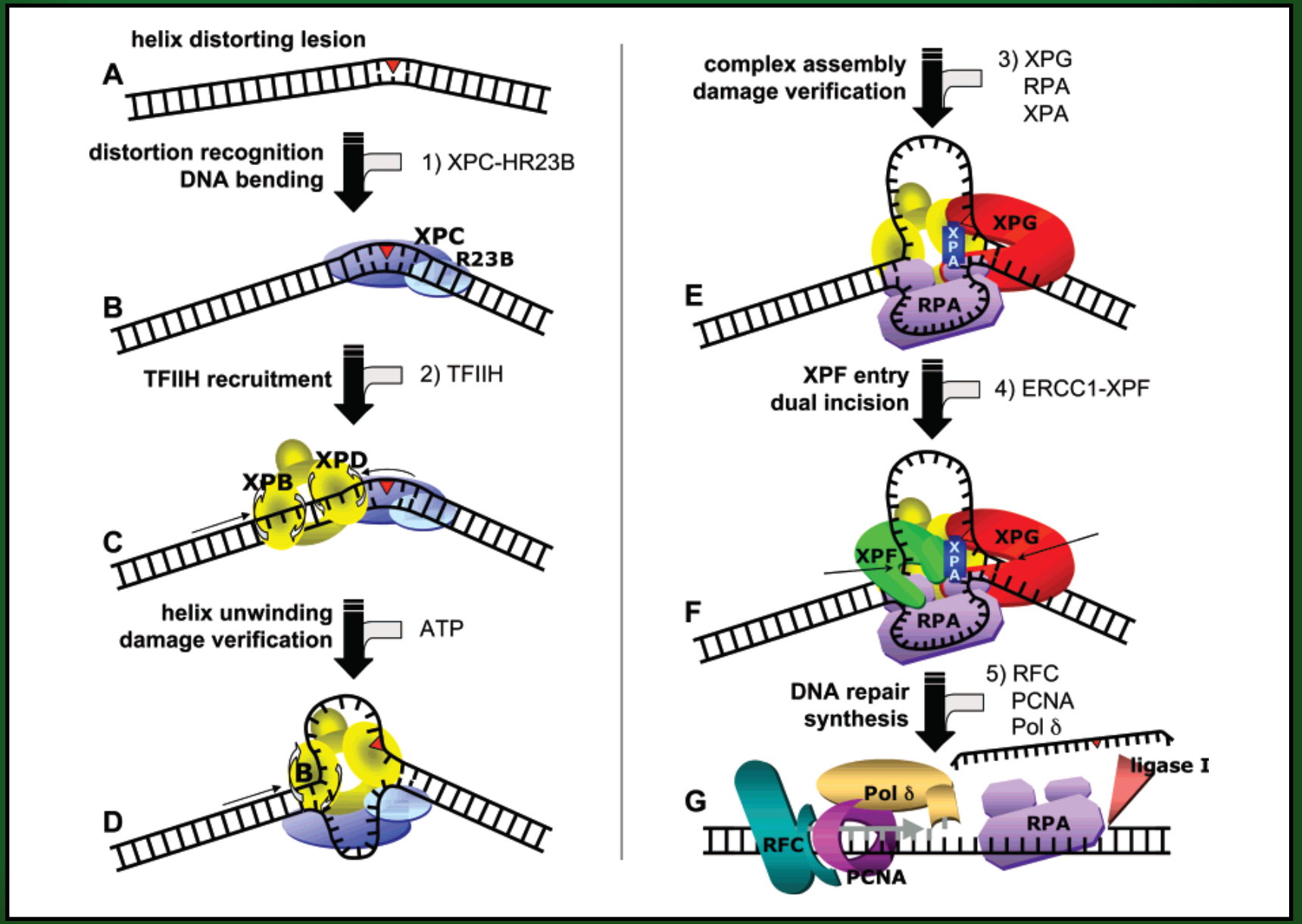

Structure of a RAD4/RAD23-CPD-DNA Complex

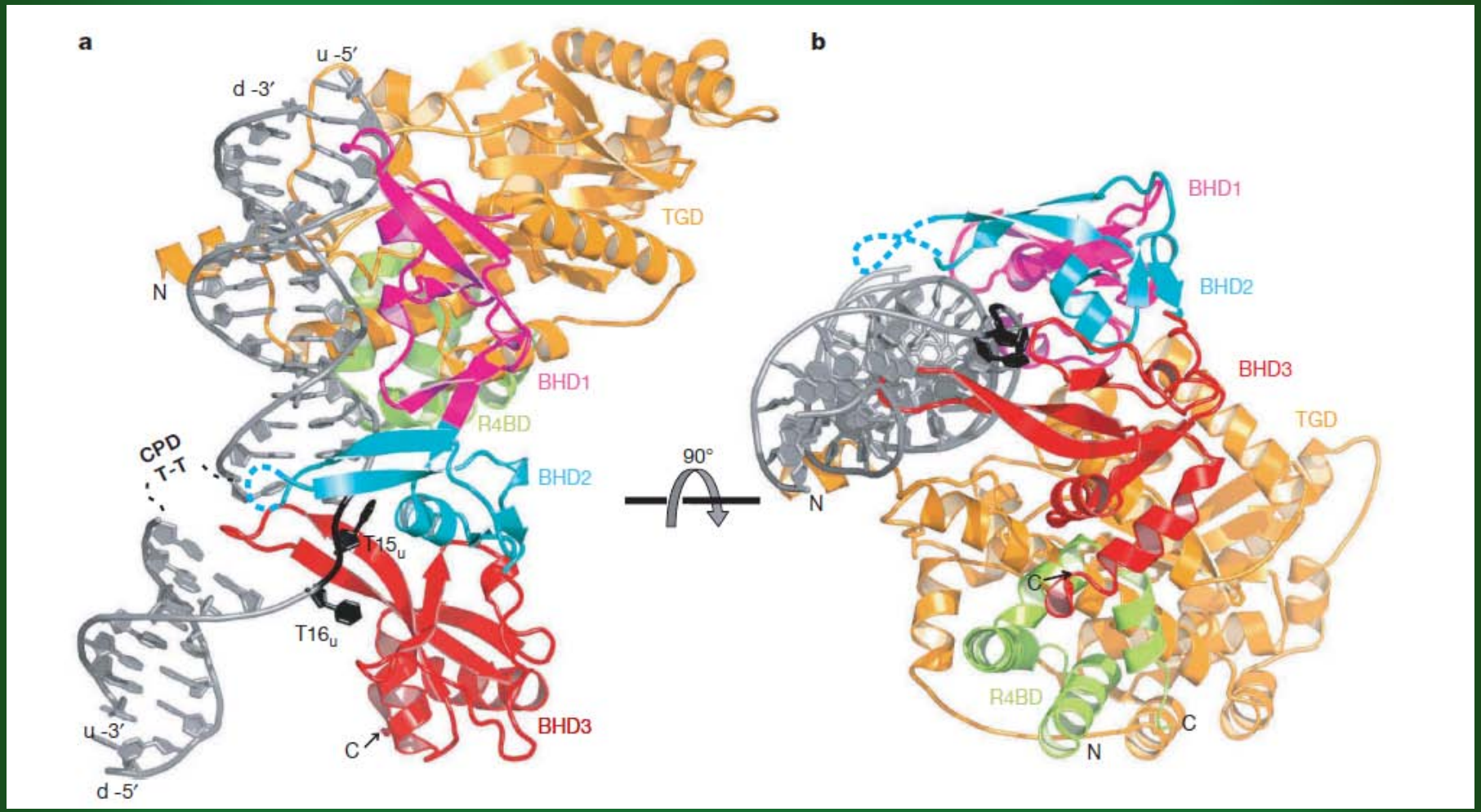

Min, J-H & Pavletich, N.P (2007) *Nature* 449, 570-576

GG-NER Resistant DNA Lesions

dG-N2 Adducts (AAF, 3ABA)

dA-N6 Adducts (ALII)

Aminofluorene

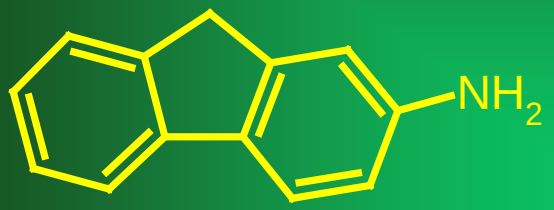

2-Aminofluorene (2-AF)

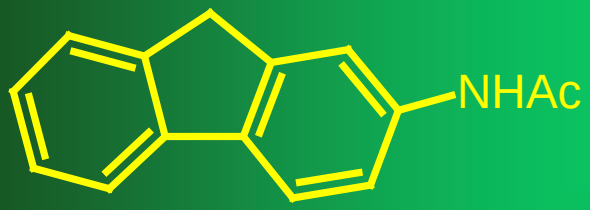

2-Acetylaminofluorene (2-AAF)

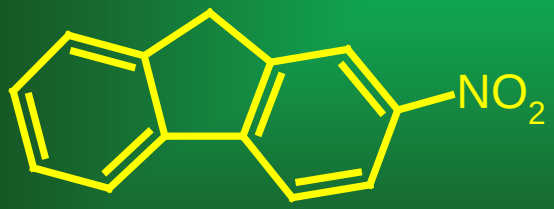

2-Nitrofluorene (2-NF)

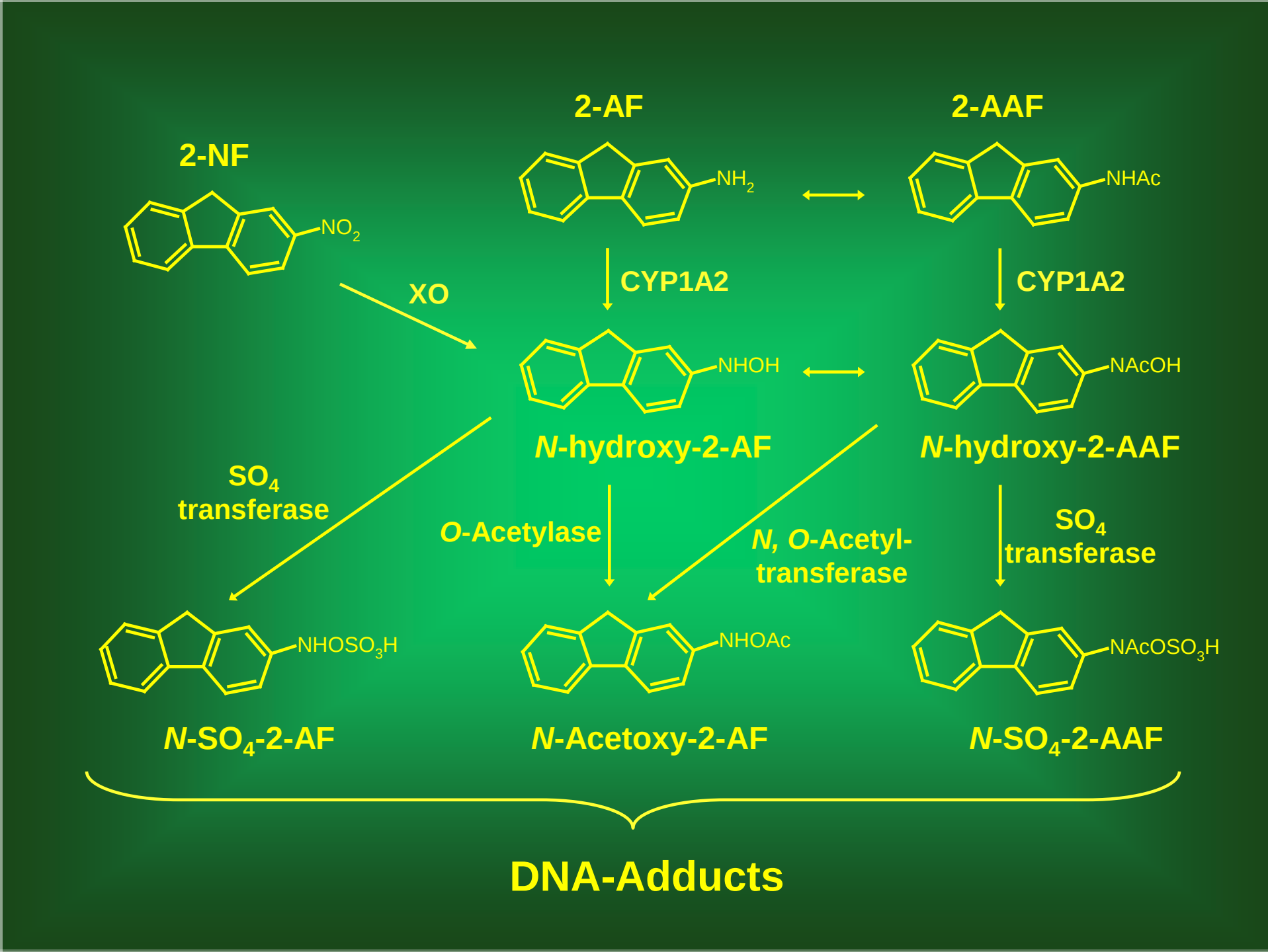
2-NF
2-AF
2-AAF
NO2
NH2
NHAc
XO
CYP1A2
CYP1A2
NHOH
NAcOH
N-hydroxy-2-AF
N-hydroxy-2-AAF
SO4 transferase
O-Acetylase
N, O-Acetyl-transferase
SO4 transferase
NHOSO3H
NHOAc
NAcOSO3H
N-SO4-2-AF
N-Acetoxy-2-AF
N-SO4-2-AAF
DNA-Adducts

DNA-Adducts

dG-C8-AF

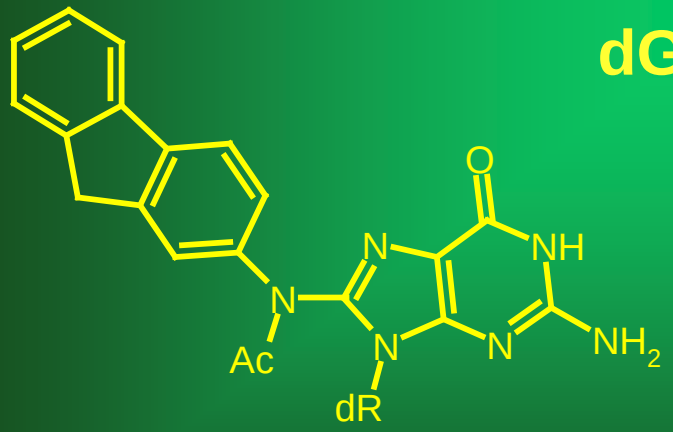

dG-C8-AAF

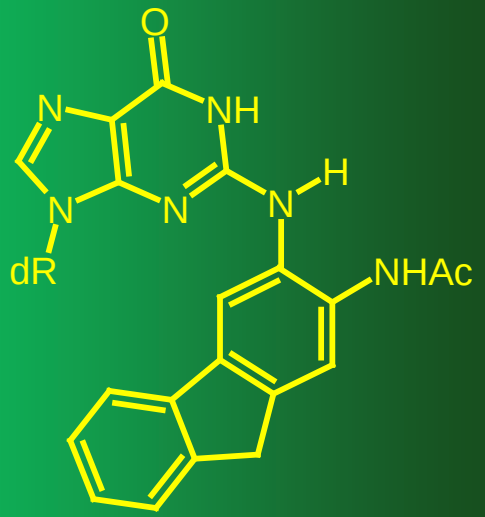

dG-*N*^{2}-AAF

dG-*N*^{2}-AAF

- Is a minor guanine adduct
- Is mutagenic: DNA-Pol I inserts dAMP, suggesting G → T mutations in bacteria
- It blocks mammalian Pol α activity *in vitro*, but TLS polymerases η and κ can bypass the lesion
- It induces G → T transversions in mammalian cells
- NER processing of dG-*N*^{2}-AAF needs full study

Formation and persistence of DNA adducts during and after a long-term administration of 2-nitrofluorene

Xian-Shu Cui [a], Lennart C. Eriksson [b], Lennart Möller [a,*]

[a] *Department of Biosciences, Center for Nutrition and Toxicology, Karolinska Institute, NOVUM Research Park, SE-141 57 Huddinge, Sweden*

Mutation Research 442 1999. 9–18

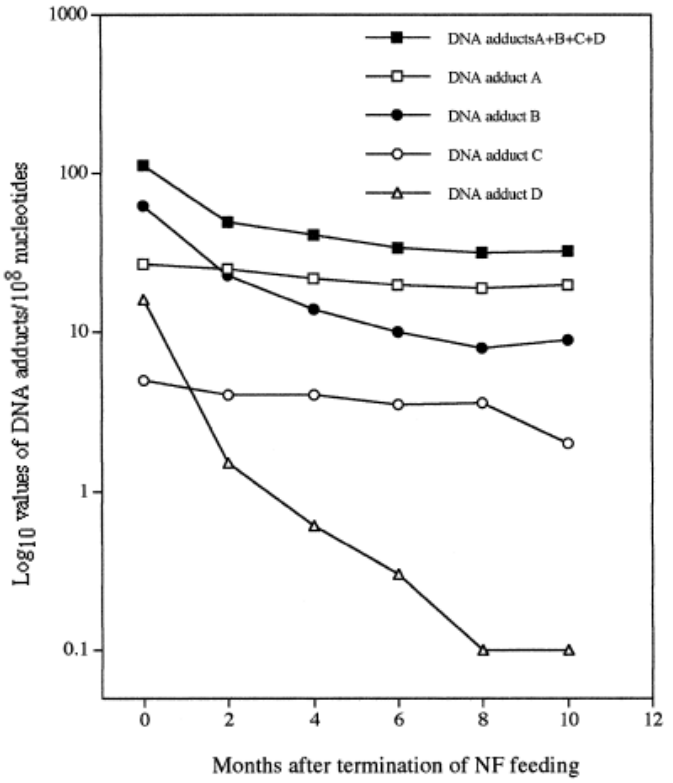

Fig. 8. The persistence of DNA adduct levels in the liver of MD rats after the termination of 11 months of NF feeding. Values showed at each time point are means of one to four samples depending on the number of rats sacrificed during that period. For further details, see Ref. [23].

- **dG-*N*²-AAF is a persistent DNA lesion**

Damaged DNA Sample

NMR Studies

NMR Constraints

Restrained MD

Structure Analysis and Validation

5′-d(C_1 G_2 T_3 A_4 C_5 X_6 C_7 A_8 T_9 G_{10} C_{11})
d(G_{22} C_{21} A_{20} T_{19} G_{18} C_{17} G_{16} T_{15} A_{14} C_{13} G_{12})-5′

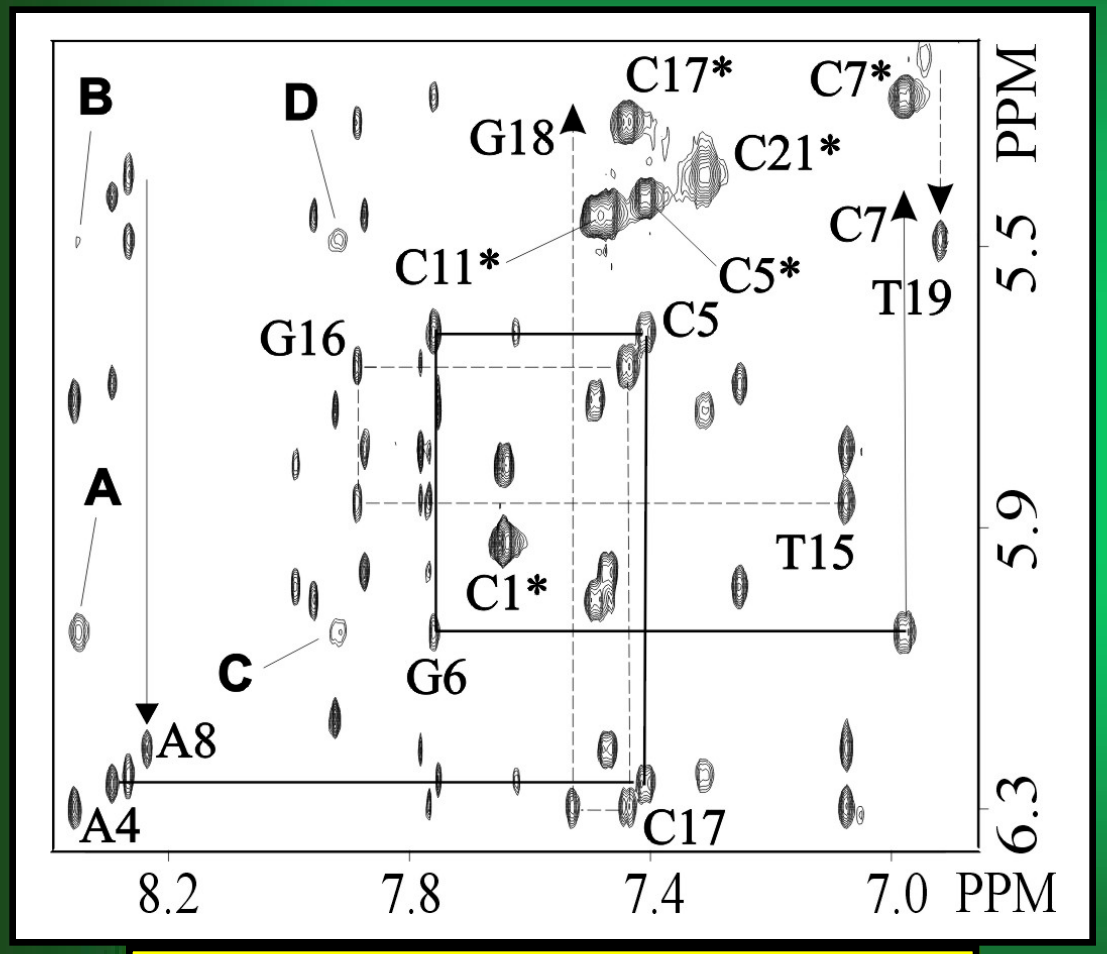

A & B, AAFH4 to G6H1′ and T19H1′
C & D, AAFH5 to G6H1′ and T19H1′

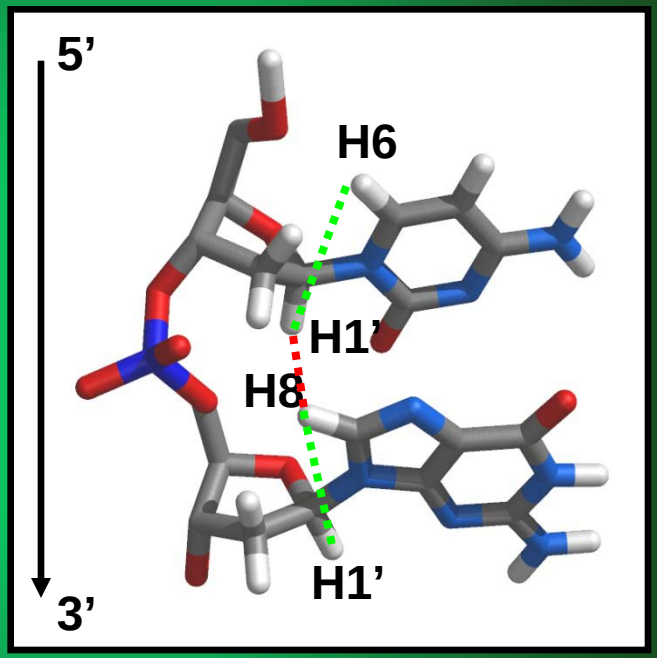

D_2O NOESY

Zaliznyak, et al. (2006) *Chem. Res. Toxicol.* **19**, 745-752.

5′-d(C_1 G_2 T_3 A_4 C_5 X_6 C_7 A_8 T_9 G_{10} C_{11})
d(G_{22} C_{21} A_{20} T_{19} G_{18} C_{17} G_{16} T_{15} A_{14} C_{13} G_{12})-5′

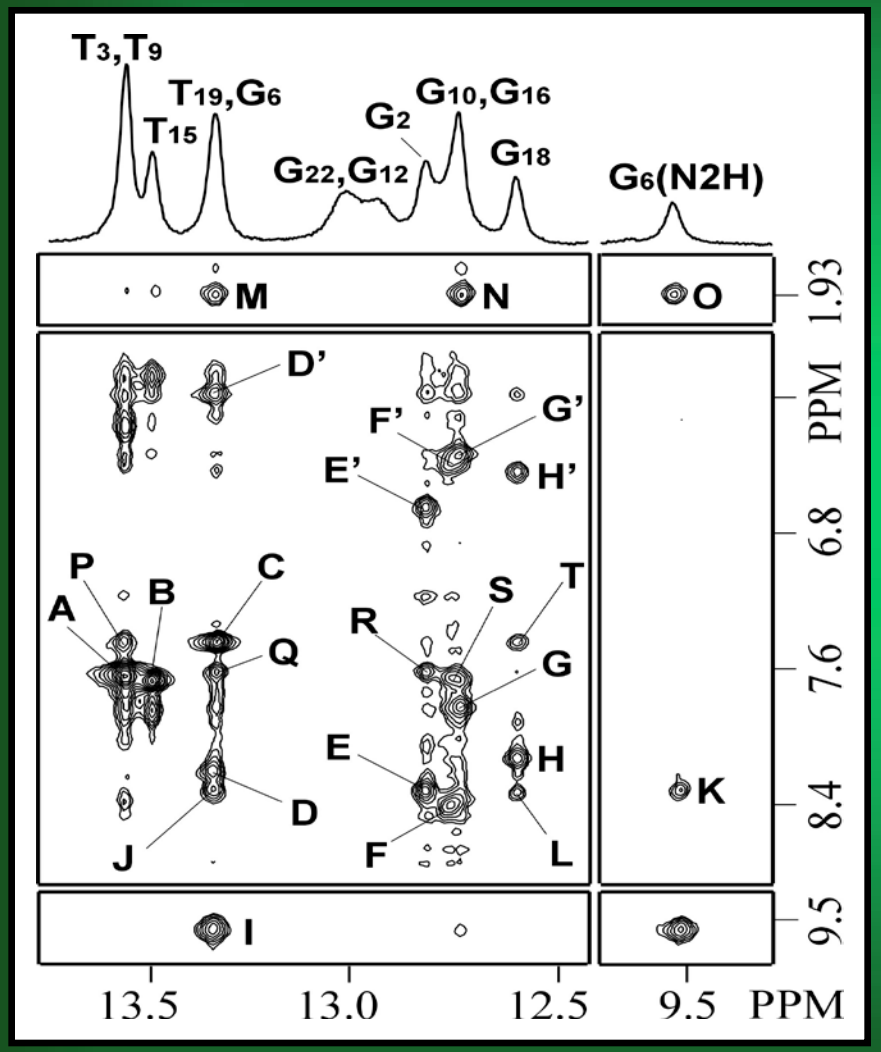

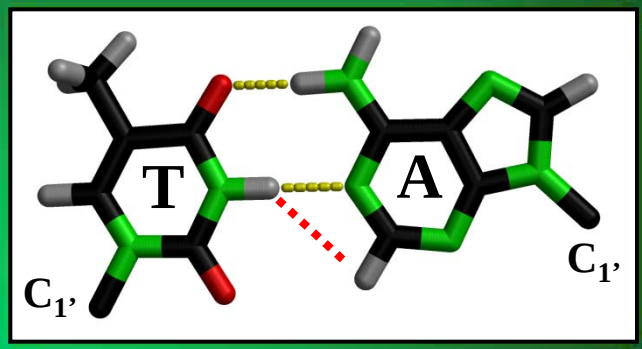

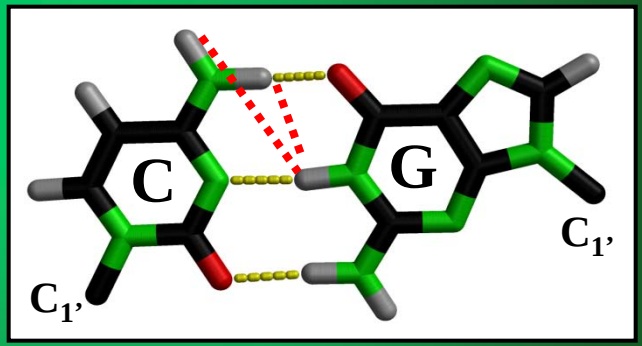

H_2O NOESY

Zaliznyak, et al. (2006) *Chem. Res. Toxicol.* **19**, 745-752.

Refined MD Structure

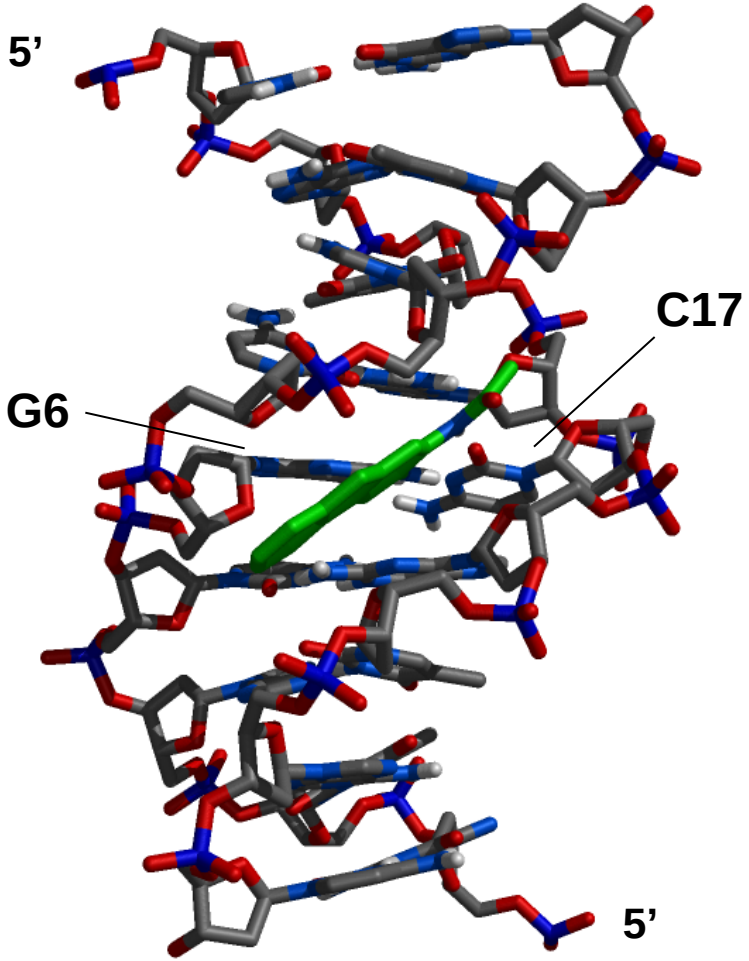

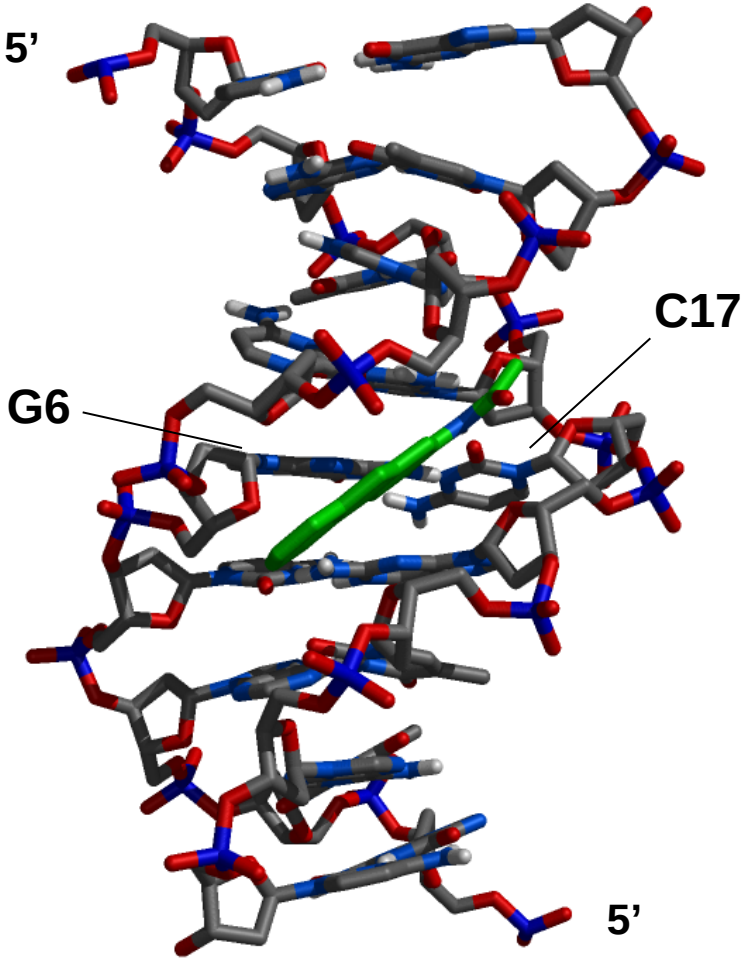

Zaliznyak, et al. (2006) *Chem. Res. Toxicol.* **19**, 745-752.

Space Filling Models

Major Groove

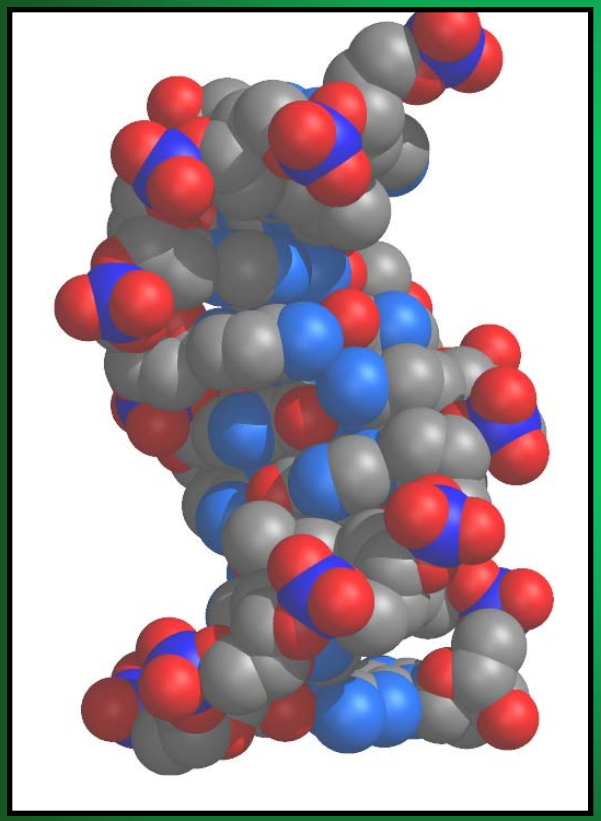

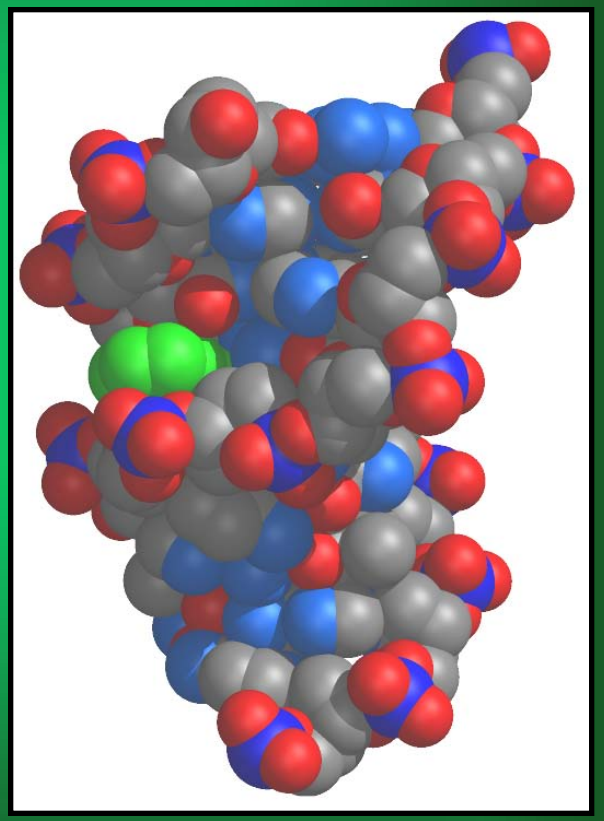

Zaliznyak, et al. (2006) *Chem. Res. Toxicol.* **19**, 745-752.

Space Filling Models

Minor Groove

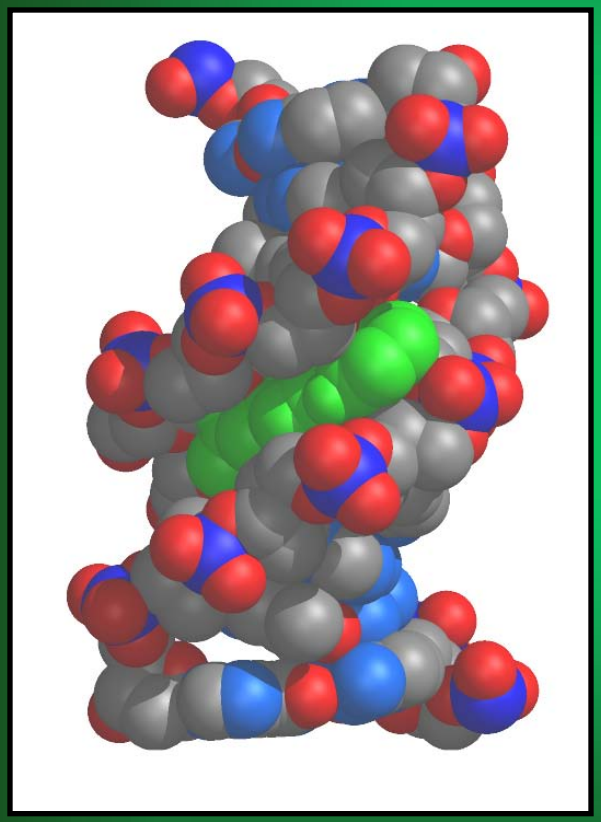

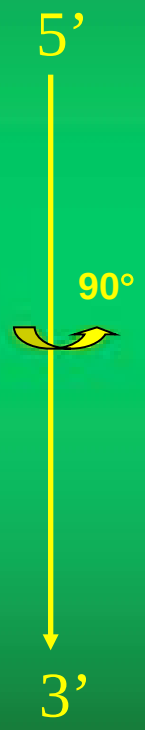

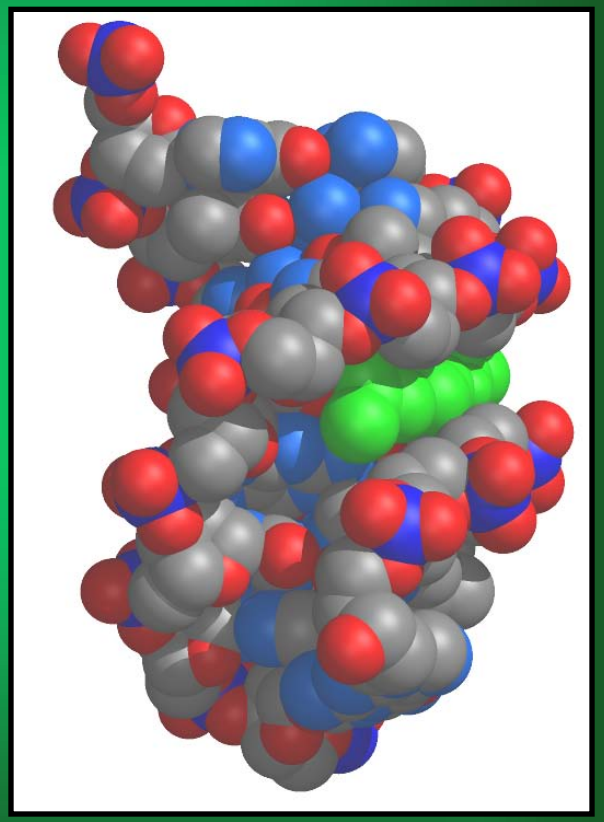

Zaliznyak, et al. (2006) *Chem. Res. Toxicol.* **19**, 745-752.

Structural Parameters

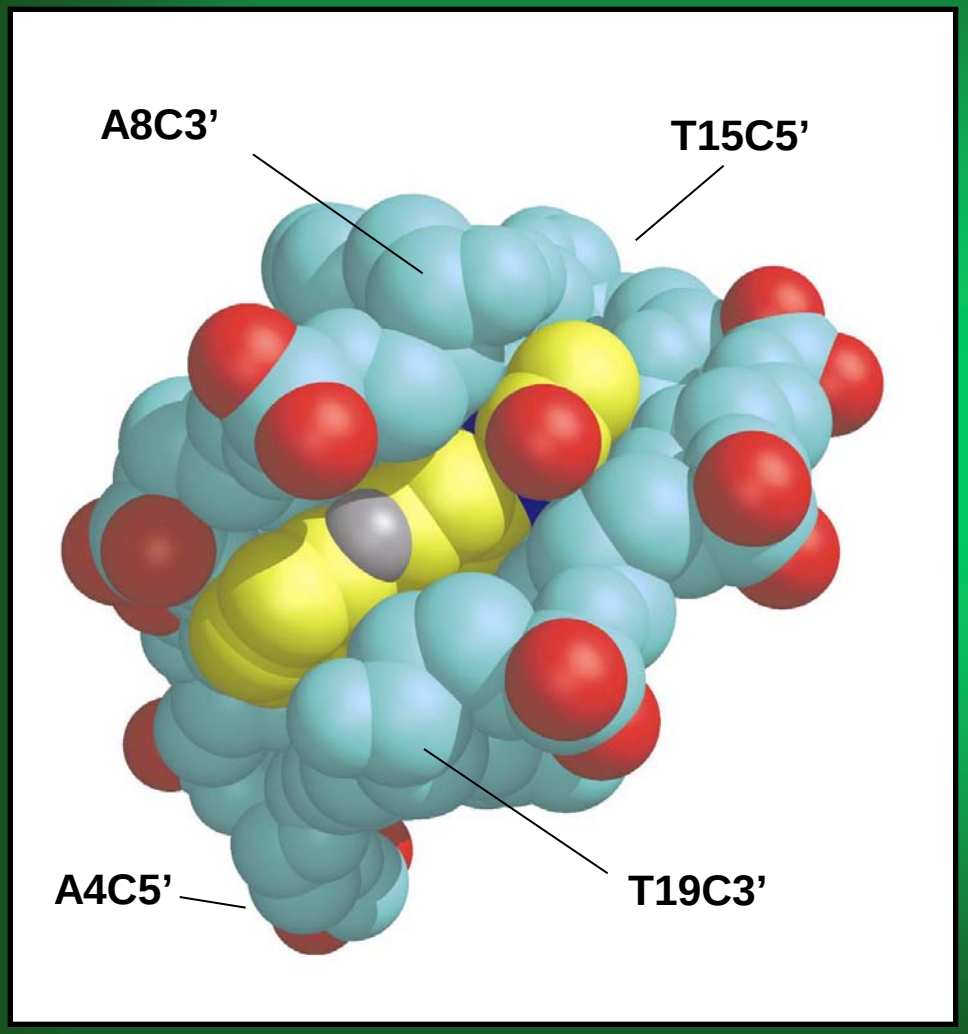

Minor groove width (Å)	2.0-4.7 (5.9)
Minor groove depth (Å)	5.6-7.2 (4.6)
BP propeller twist (°)	1-34 (<3.7)
Base pair buckle (°)	2-18 (0)
AAF Exposed Surface	17%

Zaliznyak, et al. (2006) *Chem. Res. Toxicol.* **19**, 745-752.

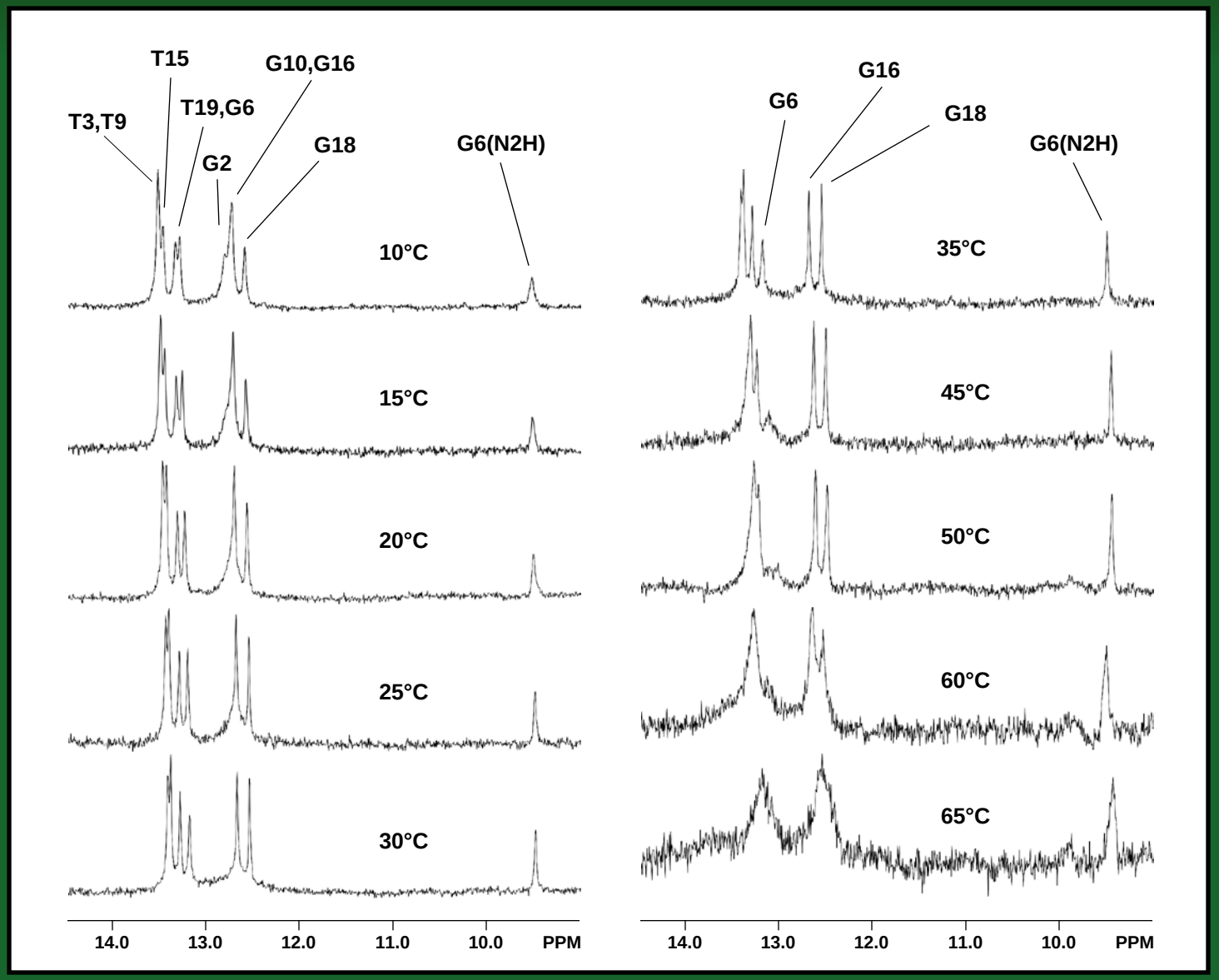

Zaliznyak, et al. (2006) *Chem. Res. Toxicol.* **19**, 745-752.

dG-N^2-AAF Duplex Stability

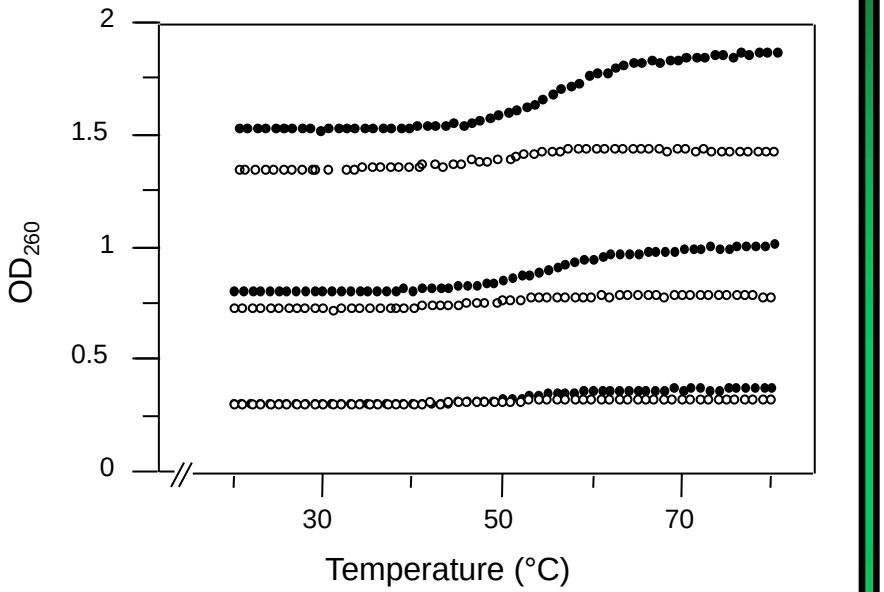

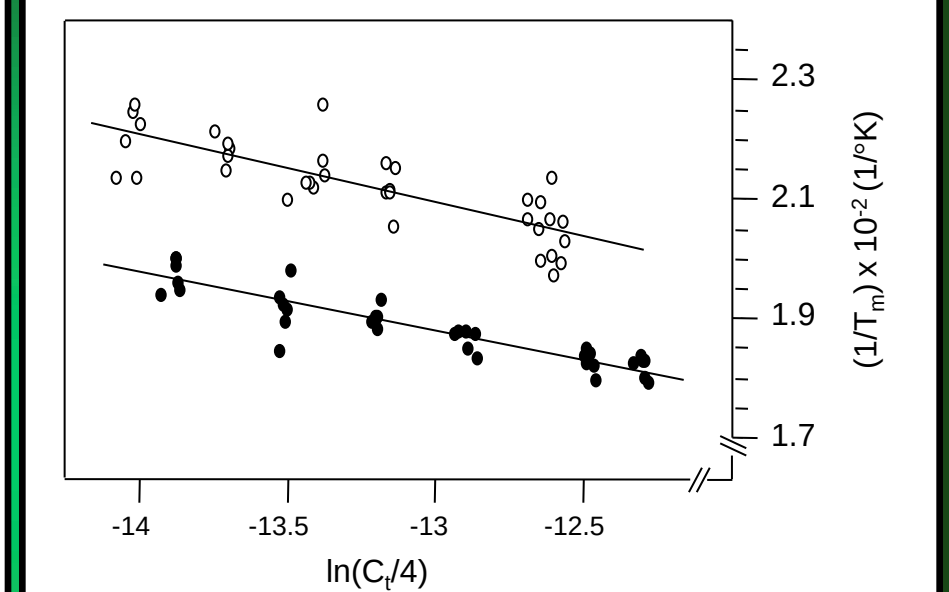

	Tm (°C)	ΔH^0 (kCal/Mol)	ΔS^0 (Cal/Mol°K)	$\Delta G^0_{25°C}$ (kCal/Mol)	$\Delta G^0_{37°C}$ (kCal/Mol)
AAF-Duplex	**60.5**	-93 ± 9	-262 ± 20	-14.9 ± 0.3	**-11.8 ± 0.3**
Control Duplex	**54.3**	-98 ± 11	-285 ± 23	-13.1 ± 0.3	**-9.6 ± 0.3**

Zaliznyak, et al. (2006) *Chem. Res. Toxicol.* **19**, 745-752.

dG-*N*^{2}-AAF Duplex

Adopts a regular helical structure with WC alignments

The lesion increases the duplex thermal and thermodynamics stability

The AAF moiety resides in the minor groove without protruding out of the helix boundaries

The minor groove deepens and narrows, sheltering AAF from water exposure

Zaliznyak, et al. (2006) *Chem. Res. Toxicol.* **19**, 745-752.

NER Repair of dG-*N*^{2}-AAF

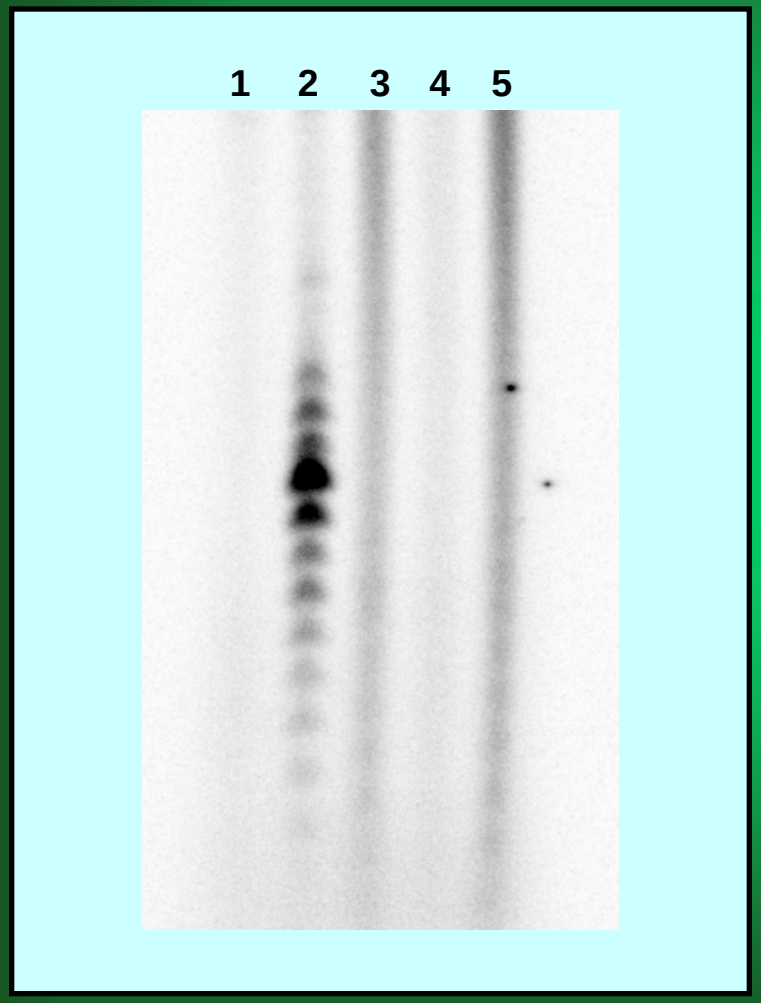

Lane 1: Hela whole cell extracts

Lane 2: Hela whole cell extracts + plasmid DNA containing a (1,3)-*N7*-*N7* *cis*-Pt adduct

Lane 3-5: Three different preparations of Hela whole cell extracts + plasmid DNA containing a dG-*N2*-AAF lesion

NER Recognition of Bulky Adducts

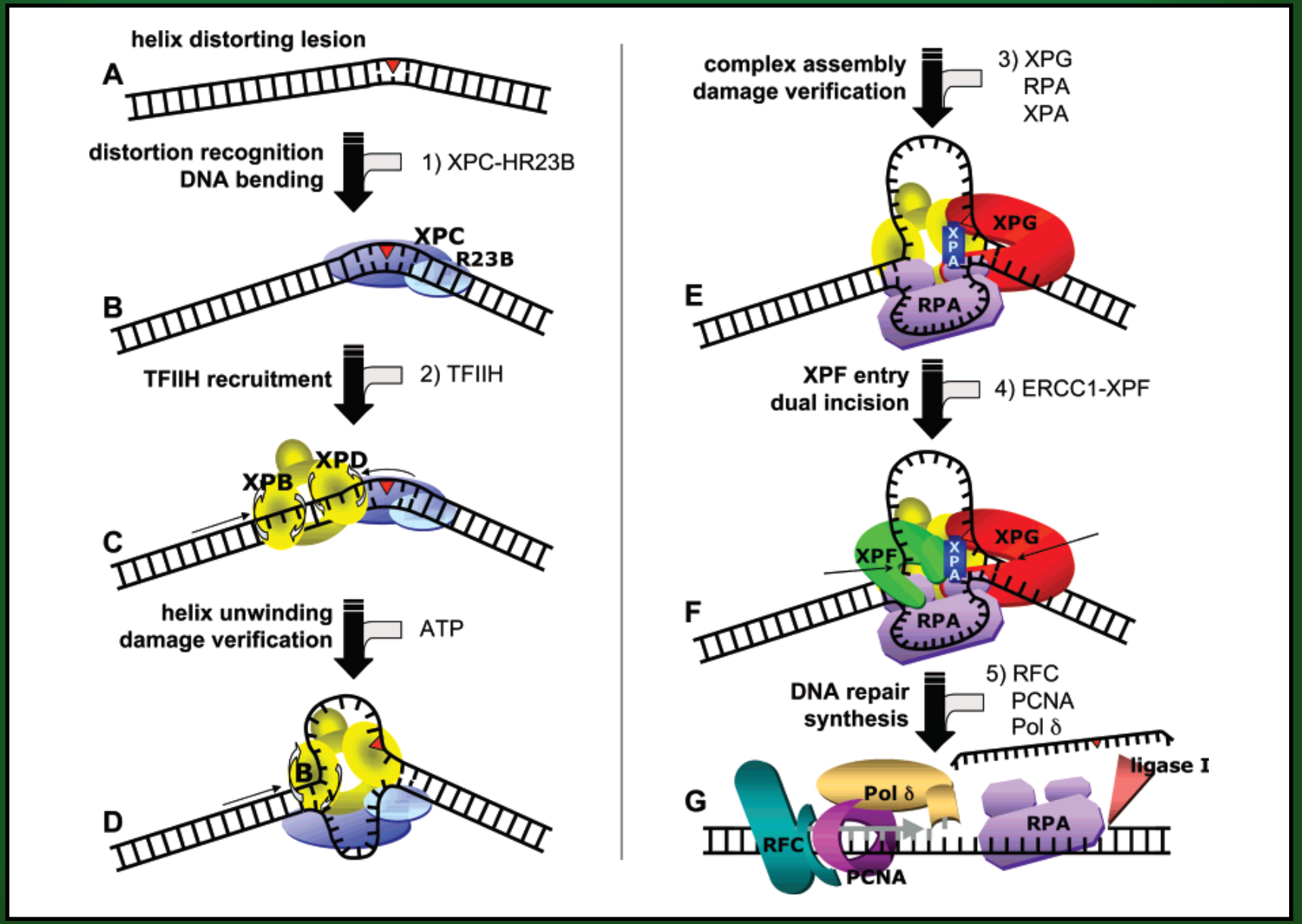

Some bulky dG-(N^2) adducts of defined topology cause minimal structural perturbations and increase duplex stability.

Thus, they evade GG-NER processing, persist in cellular DNA and are likely to have a prevalent role in chemical mutagenesis and disease.

Zaliznyak, et al. (2006) *Chem. Res. Toxicol.* **19**, 745-752.

(+) and (-) *trans*-benzo[a]pyrene-N2-dG Lesions

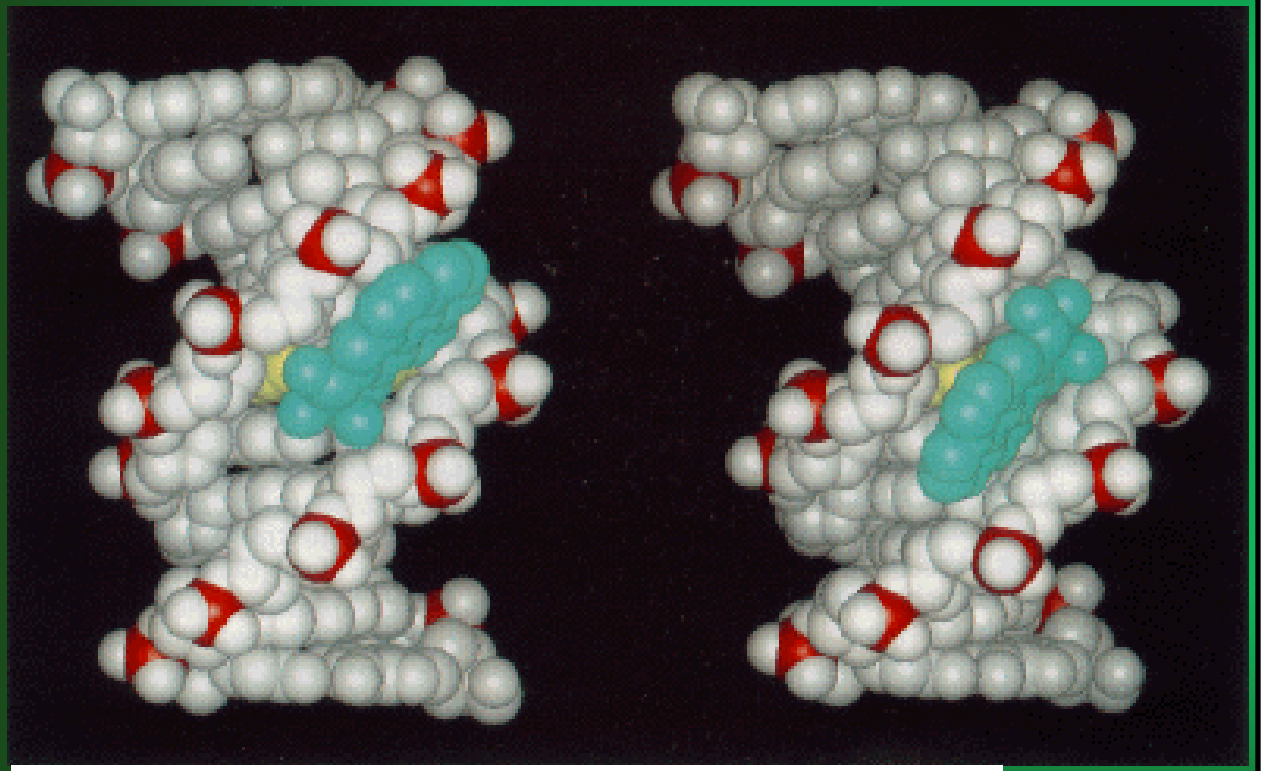

Cosman, et al. (1992) *Proc. Natl. Acad. Sci. USA* **89**, 1914-1918.
de los Santos, et al. (1992) *Biochemistry.* **31**, 5245-5252.

AAF-N2-dG Lesions

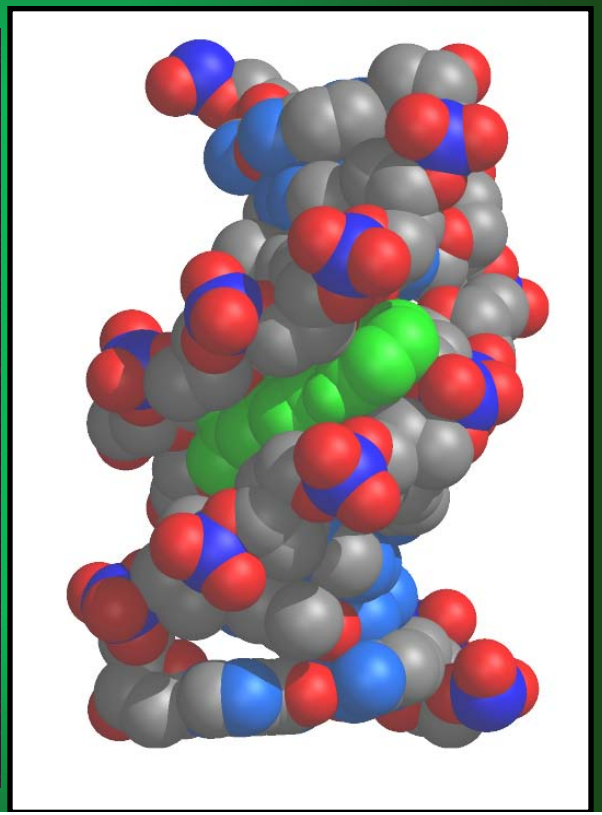

Zaliznyak, et al. (2006) *Chem. Res. Toxicol.* **19**, 745-752.

Topology of helix-stabilizing lesions

dG-*N*^{2}-AAF

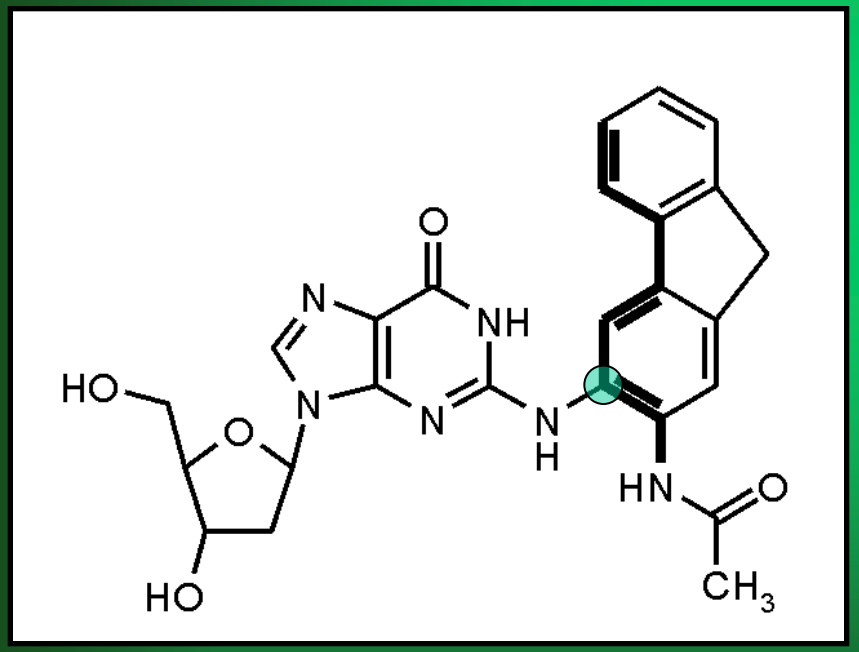

dG-*N*^{2}-3ABA

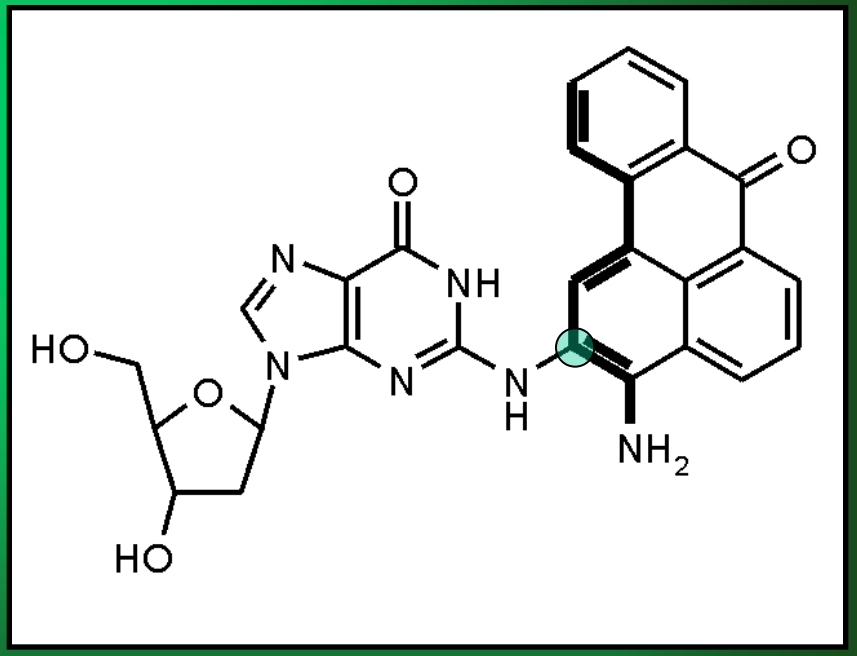

3-Nitrobenzanthrone

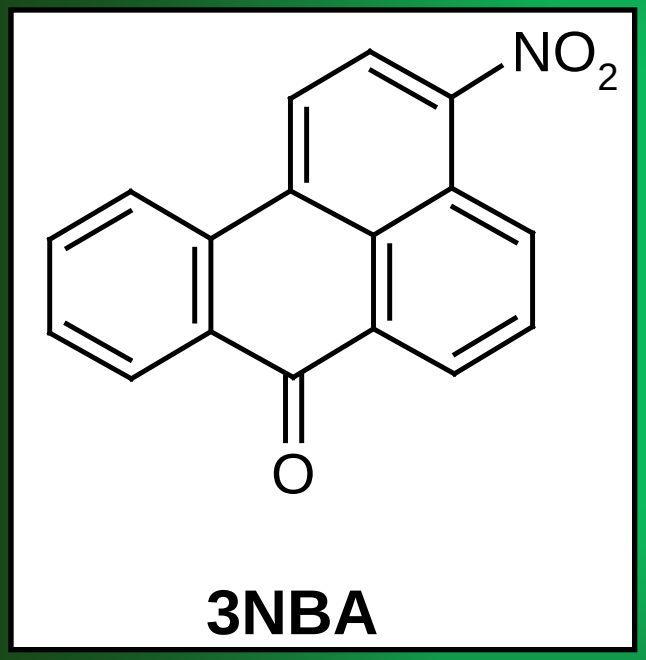

3NBA

Present in coal fly ash, diesel engine exhausts and air particulate matter

Strong mammalian mutagen

Causes DSB and induces micronuclei formation in human cells

Causes squamous cell lung tumors in rats.

Epidemiologically linked to lung cancer in humans

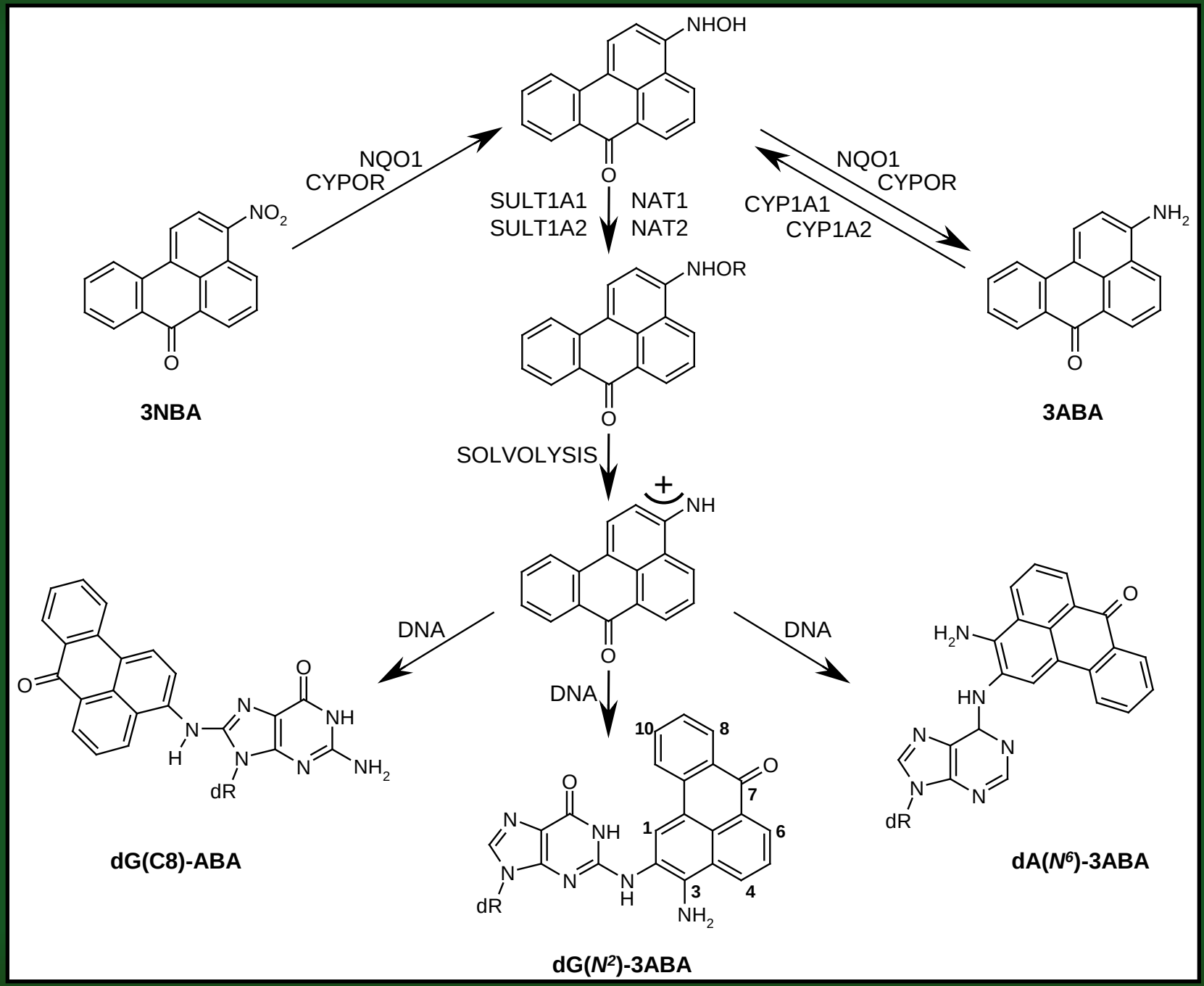
NHOH
O
NQO1
CYPOR
SULT1A1
SULT1A2
NAT1
NAT2
NQO1
CYPOR
CYP1A1
CYP1A2
NO2
NHOR
NH2
3NBA
3ABA
SOLVOLYSIS
NH
DNA
DNA
DNA
dG(C8)-ABA
dG(N2)-3ABA
dA(N6)-3ABA
dR
H2N
HN
NH2
10
8
7
6
1
3
4

Scheme 1. Synthesis of protected dG(N^2)-3ABA phosphoramidite

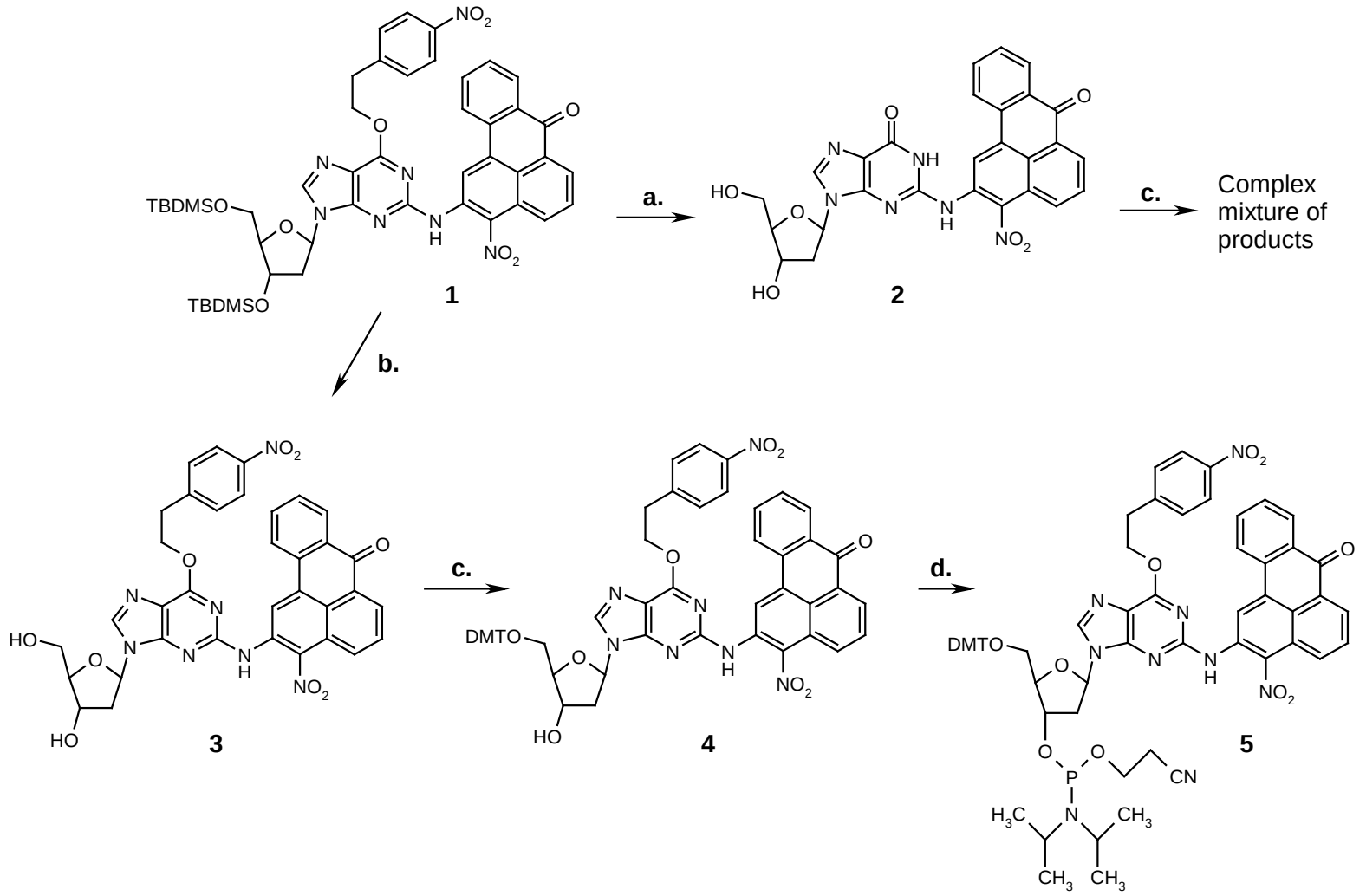

a. 1M tetrabutylammonium fluoride, THF; b. Triethylamine trihydrofluoride:triethylamine:DMF (4:3:6);
c. Dimethoxytrityl chloride, pyridine; d. Cyanoethoxy diisopropylamino chlorophosphine.

Lukin, et al. (2011) *J. Nucleic Acids* Epub 2011 Nov 17.

Scheme 2. Deprotection and nitro reduction of dG(N^2)-NBA in oligonucleotides

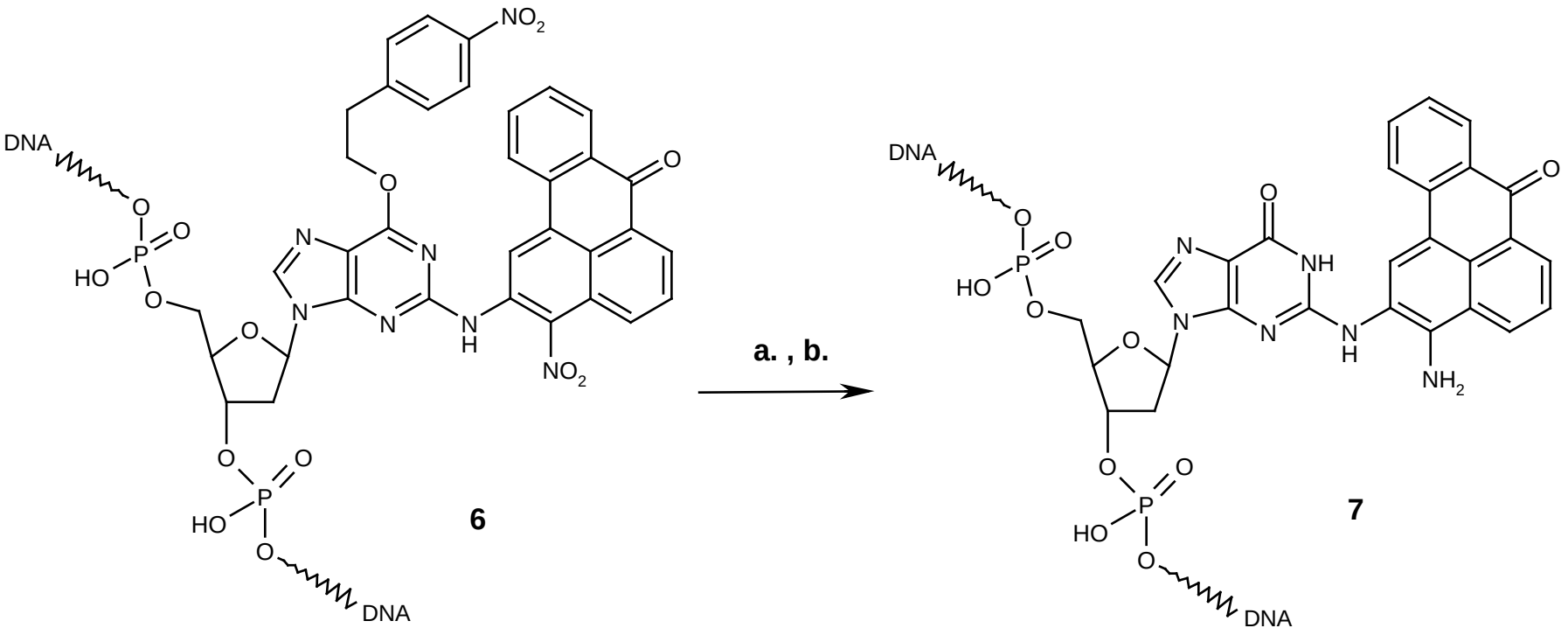

a.1M tetrabutylammonium fluoride, THF; b. 1M Na_2S.

G_1 T_2 A_3 T_4 X_5 C_6 C_7 G_8 G_9 C_{10} A_{11} T_{12} A_{13} C_{14}

Lukin, et al. (2011) *J. Nucleic Acids* Epub 2011 Nov 17.

dG-(N^2)-3ABA Duplex

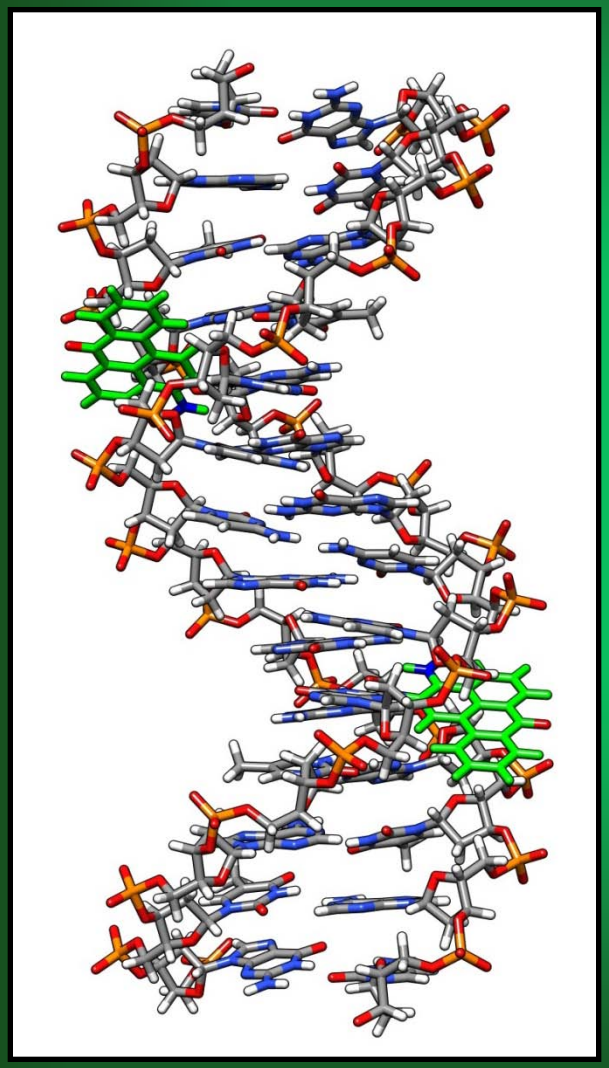

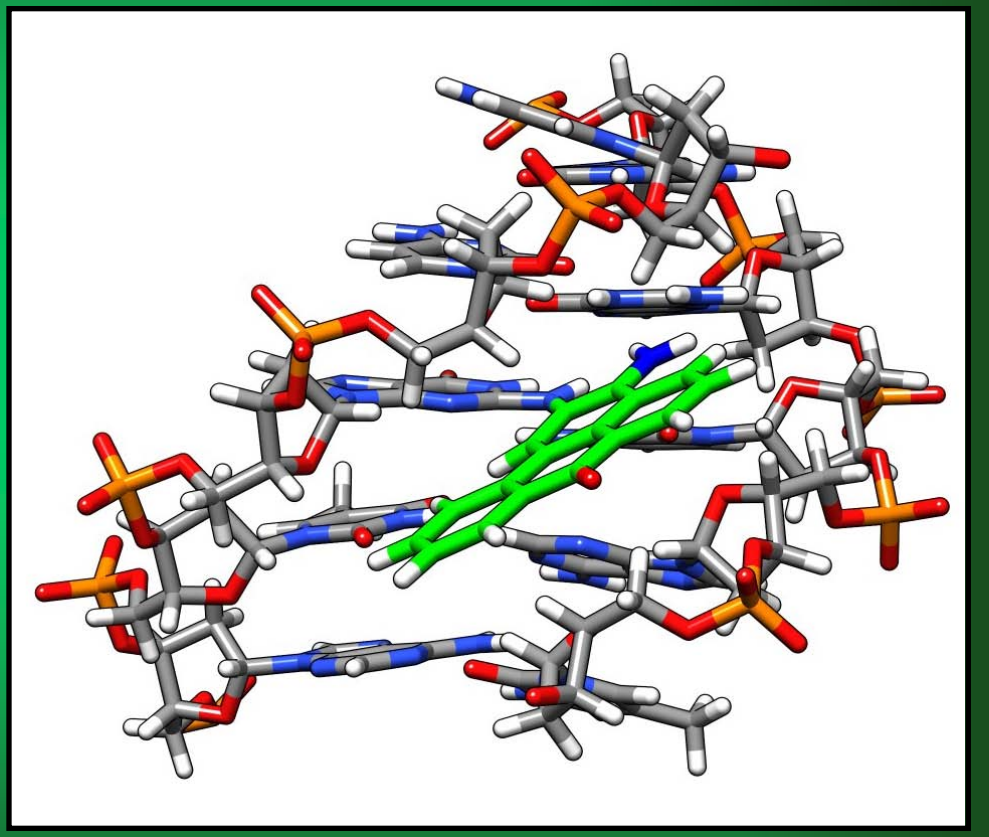

dG-(N^2)-3ABA Duplex

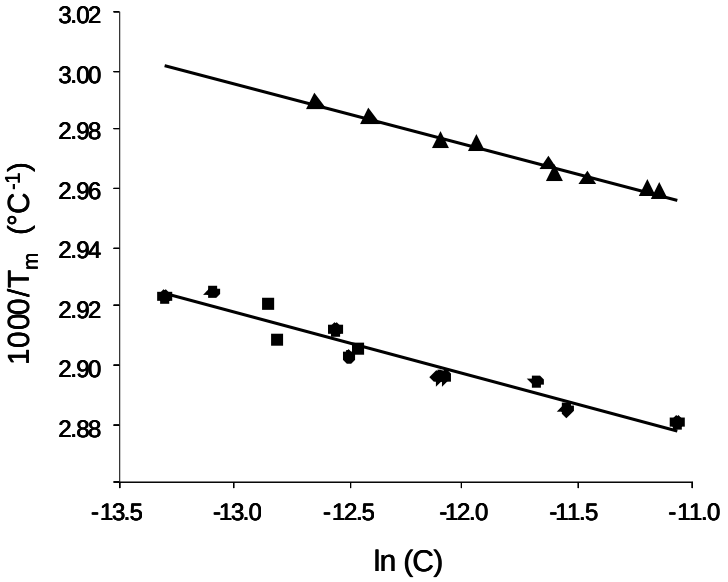

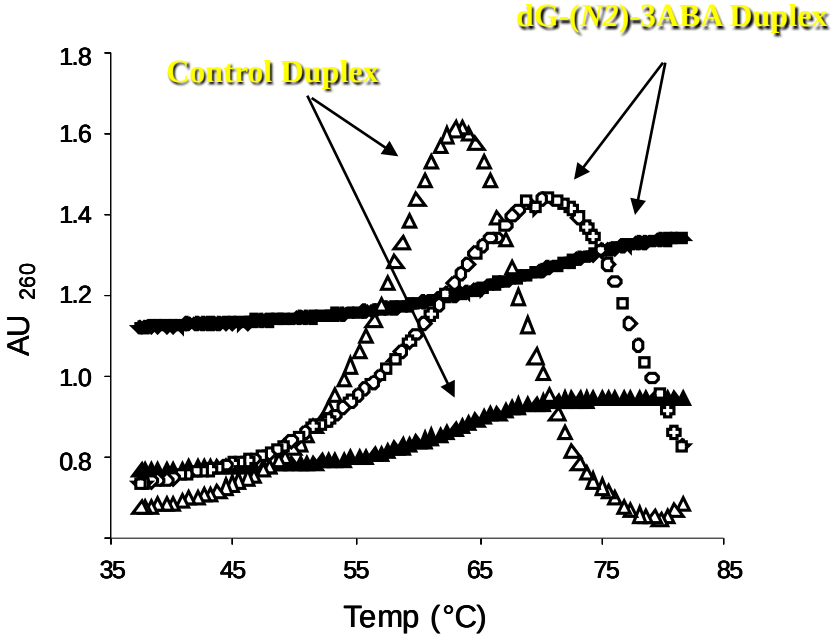

	ΔH°_{25}, kcal/mol	ΔS°_{25}, cal/mol·K	ΔG°_{25}, kcal/mol	ΔG°_{37}, kcal/mol	$\Delta\Delta G^\circ_{37/lesion}$, kcal/mol
dG(^{2}N)-ABA duplex	-95 ± 8	-252 ± 24	-21 ± 1.1	-17.9 ± 0.8	-1.5
Control duplex	-98 ± 4	-267 ± 11	-18.2 ± 0.5	-14.9 ± 0.3	

dG-*N*^{2}-AAF

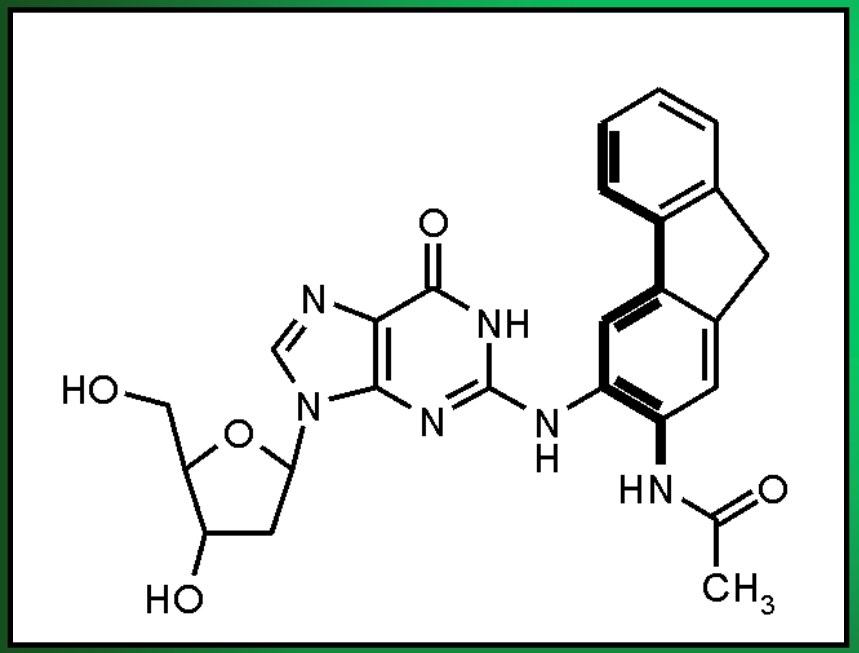

dG-*N*^{2}-3ABA

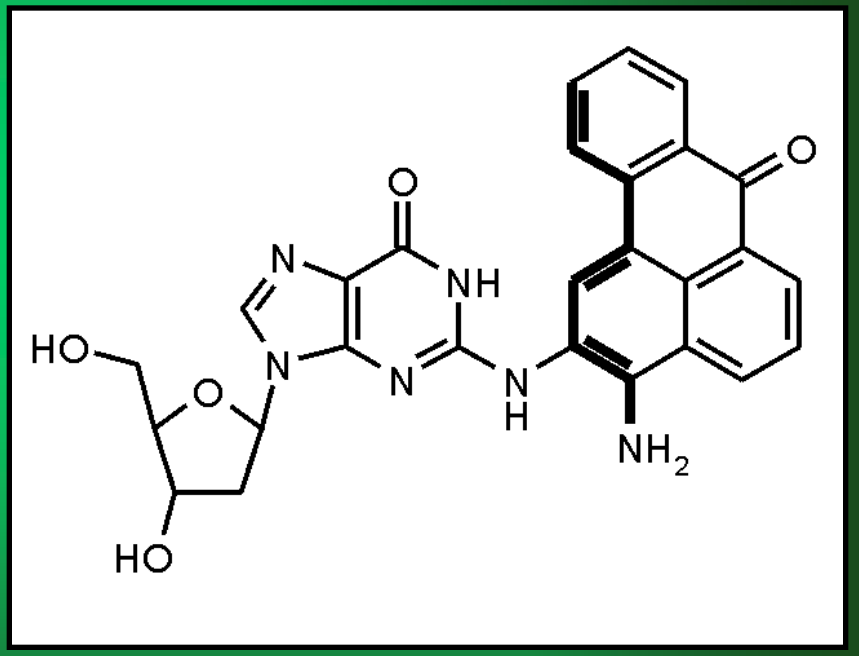

NER Recognition of Bulky Adducts

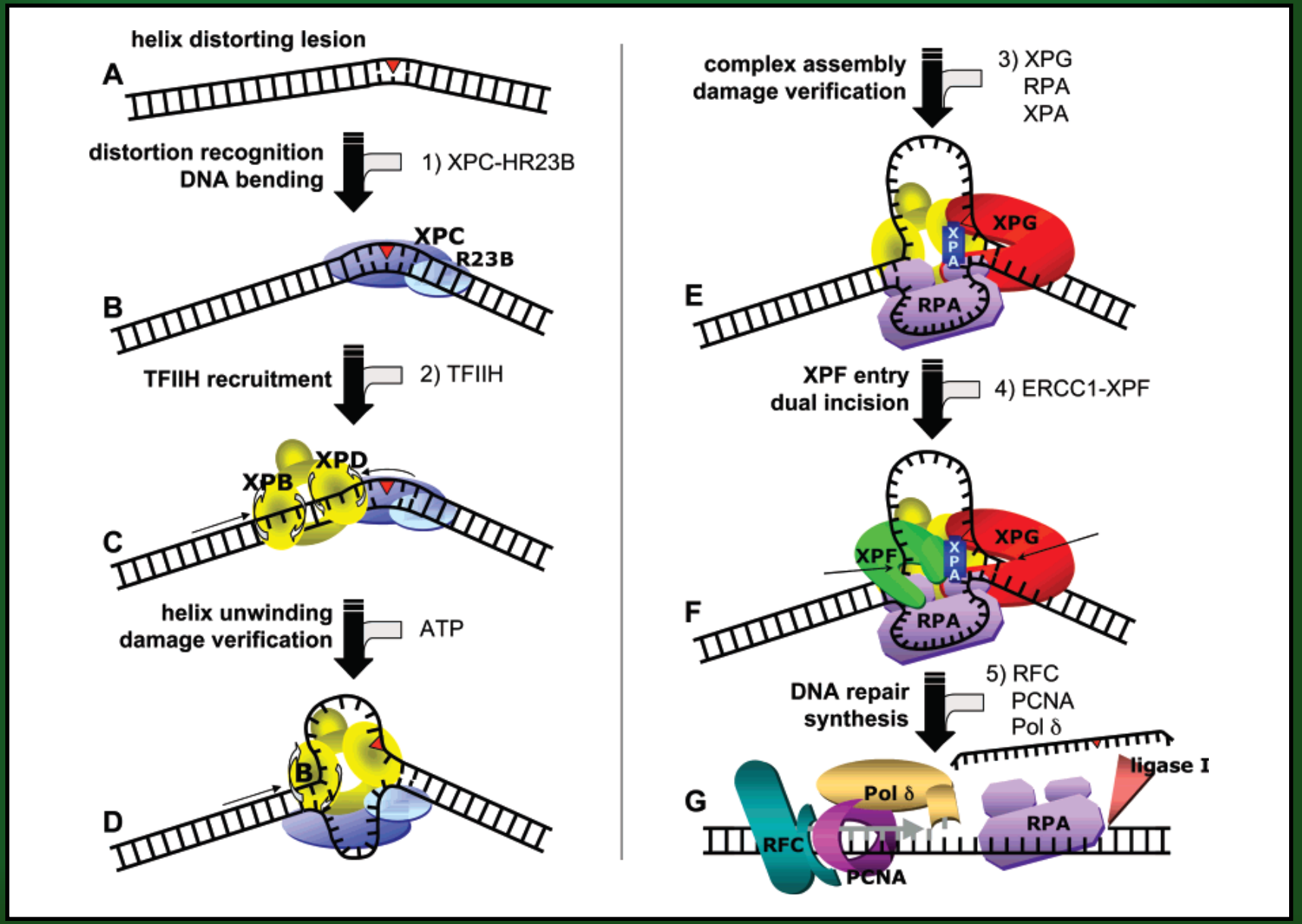

Aristolochic Acids

Aristolochia elegans

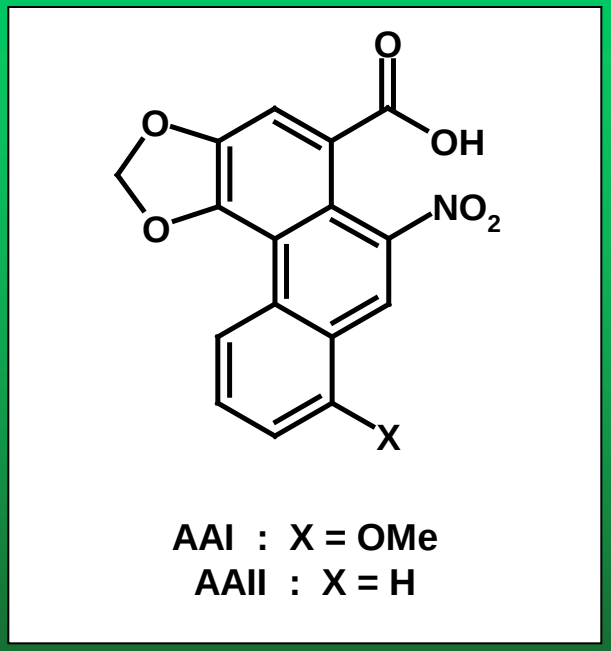

AAI : X = OMe
AAII : X = H

Aristolochia clematitis

AA-I is nephrotoxic: causes interstitial fibrosis with progression to end-stage renal disease
Many patients develop urothelial cancer

Both AA-I & AA-II are genotoxic, mostly leading to AT → TA transversions

AA-dA adducts persist in chromosomal DNA for several years

The National Toxicology Program listed the AAs as established human carcinogens

Aristolochic Acids

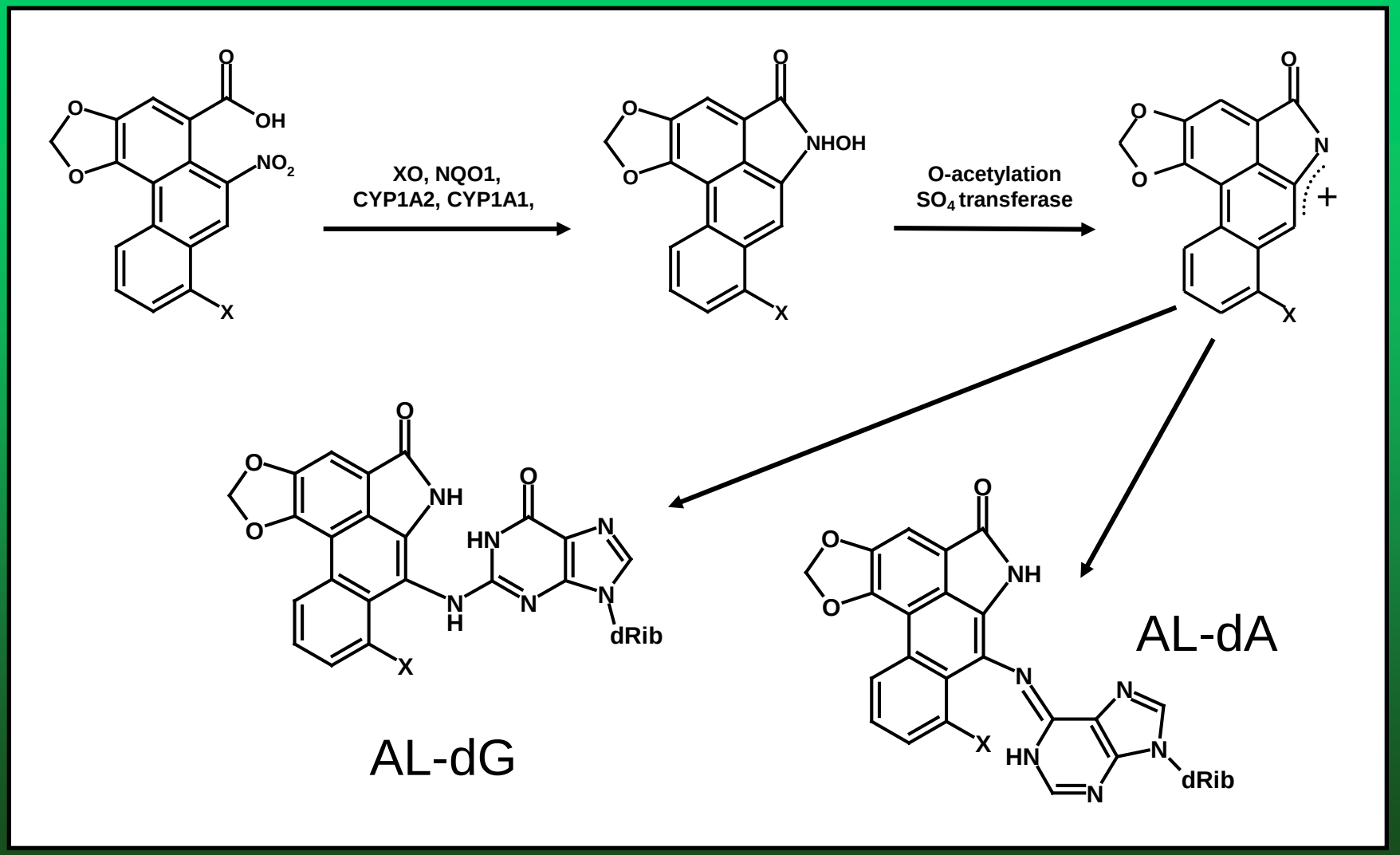

dA-(N^6)-ALII Duplex

C1	G2	T3	A4	C5	X6	C7	A8	T9	G10	C11
G22	C21	A20	T19	G18	T17	G16	T15	A14	C13	G12

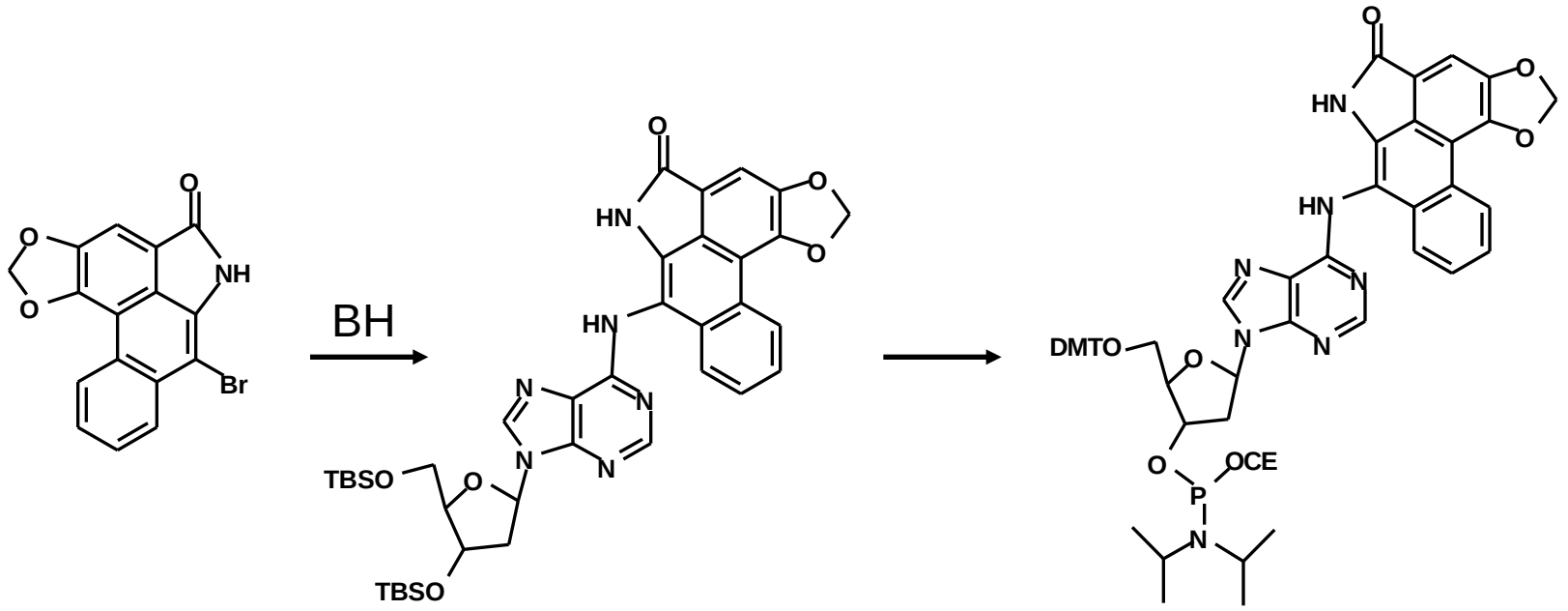

Attaluri et al. (2010) *Nucleic Acids Res.*, **38**, 339-352.

dA-(N^6)-ALII Duplex

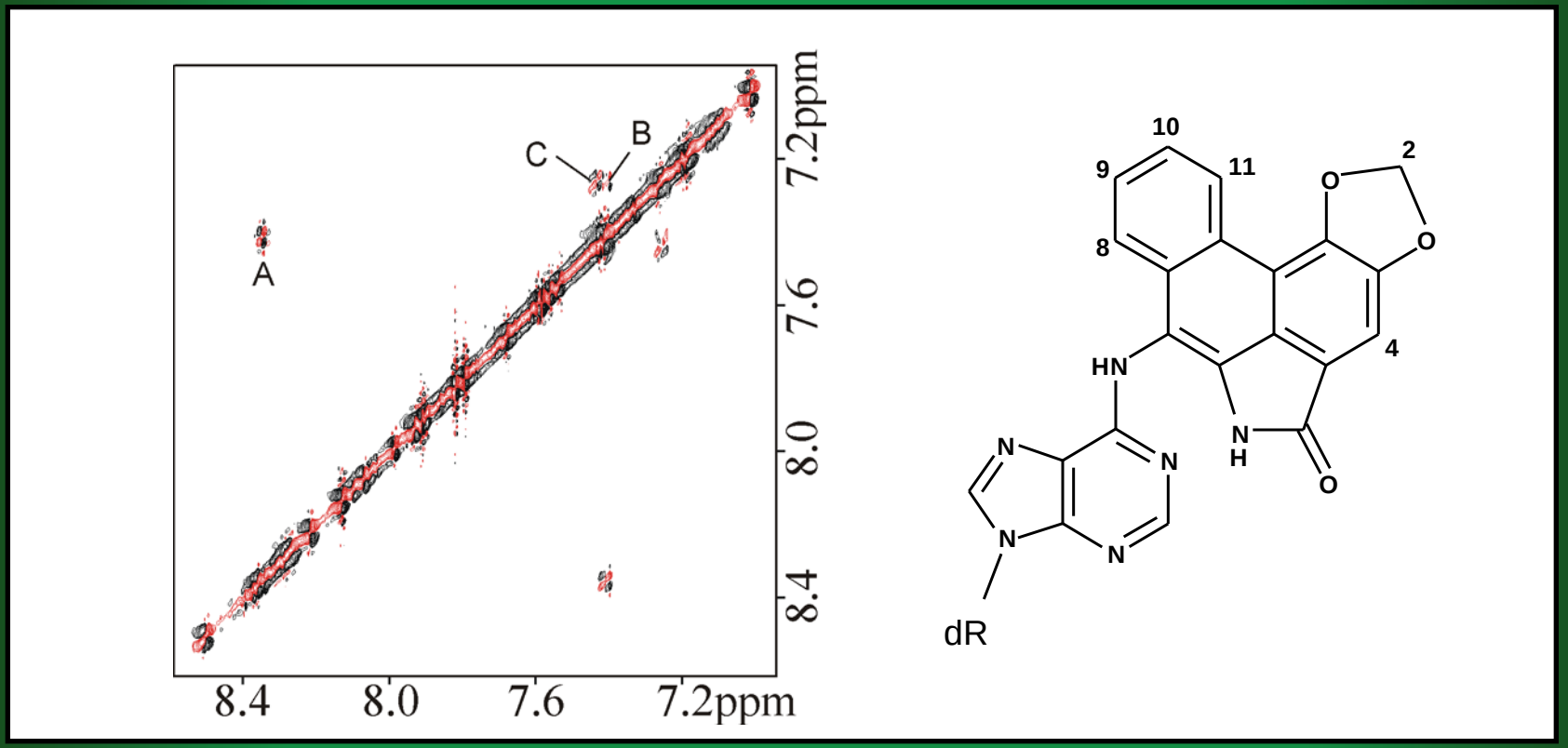

A) AAH11-AAH10 B) AAH10-AAH9 C) AAH8-AAH9

Lukin et al (2012) *Nucleic Acids Res.* 2012 40, 2759-2770.

dA-(N^6)-ALII Duplex

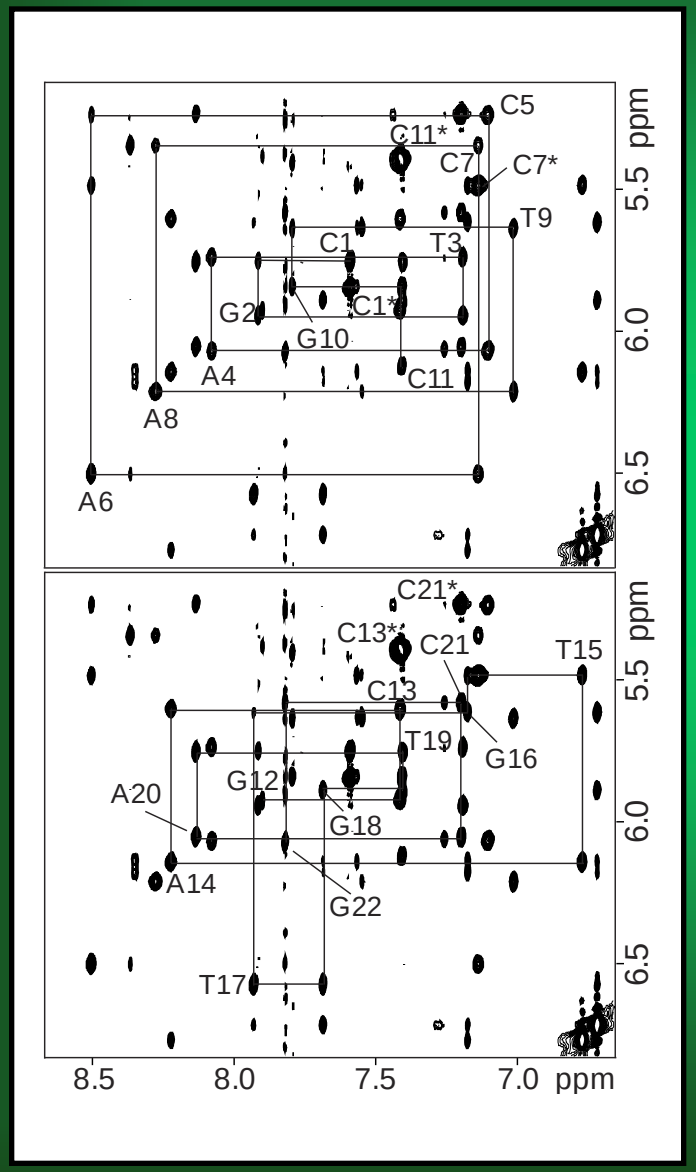

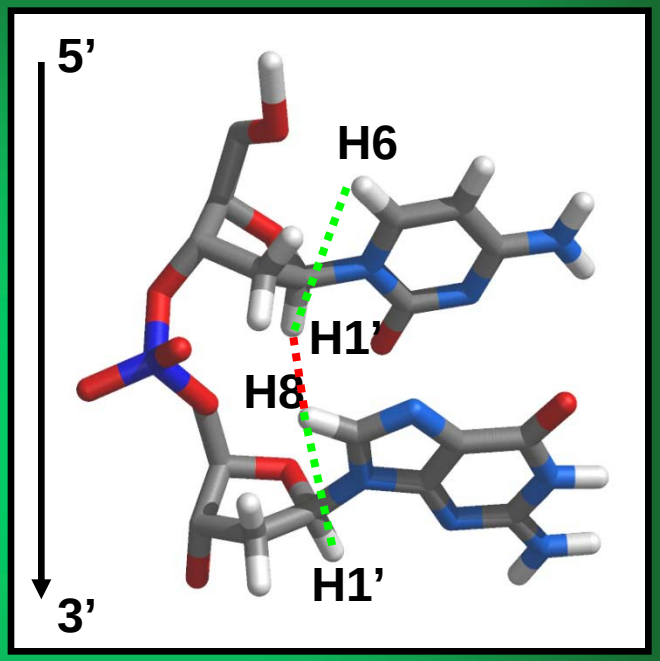

D_2O NOESY

Lukin et al (2012) *Nucleic Acids Res.* 2012 40, 2759-2770.

dA-(N^6)-ALII Duplex

C_1	G_2	T_3	A_4	C_5	X_6	C_7	A_8	T_9	G_{10}	C_{11}
G_{22}	C_{21}	A_{20}	T_{19}	G_{18}	T_{17}	G_{16}	T_{15}	A_{14}	C_{13}	G_{12}

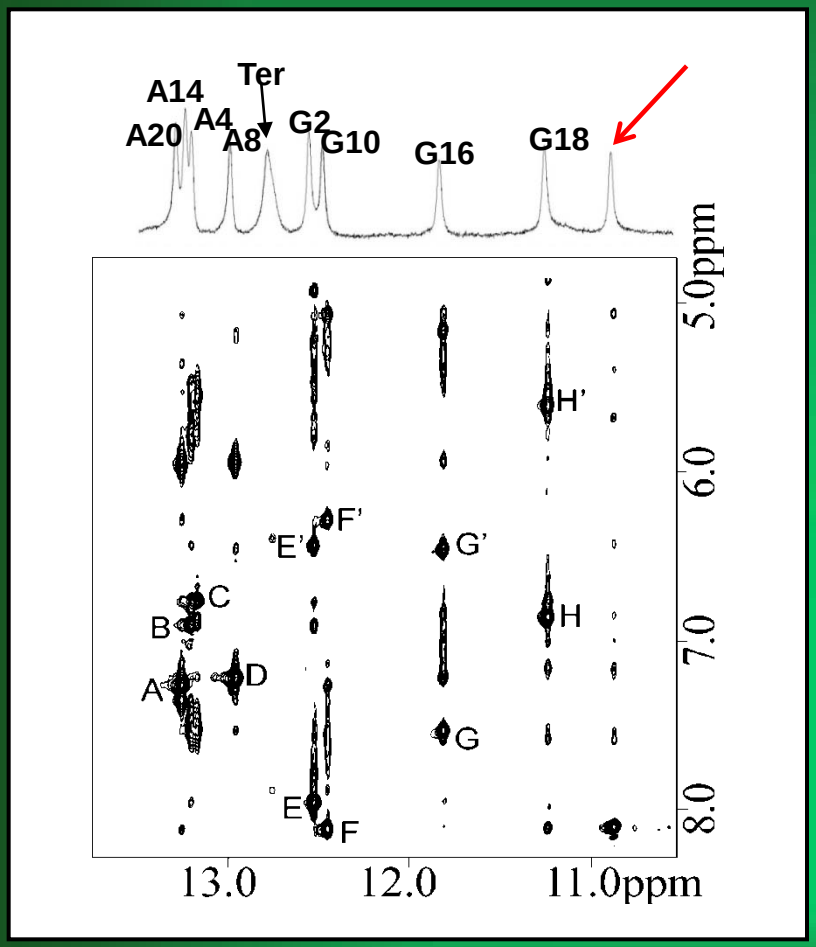

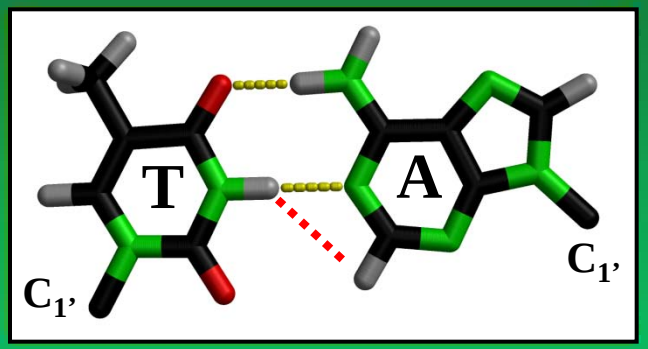

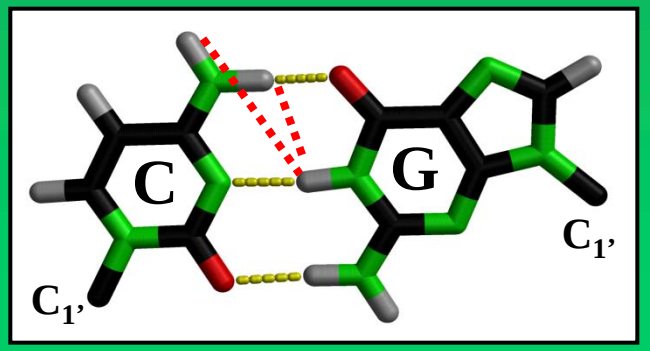

H_2O NOESY

Lukin et al (2012) *Nucleic Acids Res.* 2012 40, 2759-2770.

dA-(N^6)-ALII Duplex

C_1	G_2	T_3	A_4	C_5	X_6	C_7	A_8	T_9	G_{10}	C_{11}
G_{22}	C_{21}	A_{20}	T_{19}	G_{18}	T_{17}	G_{16}	T_{15}	A_{14}	C_{13}	G_{12}

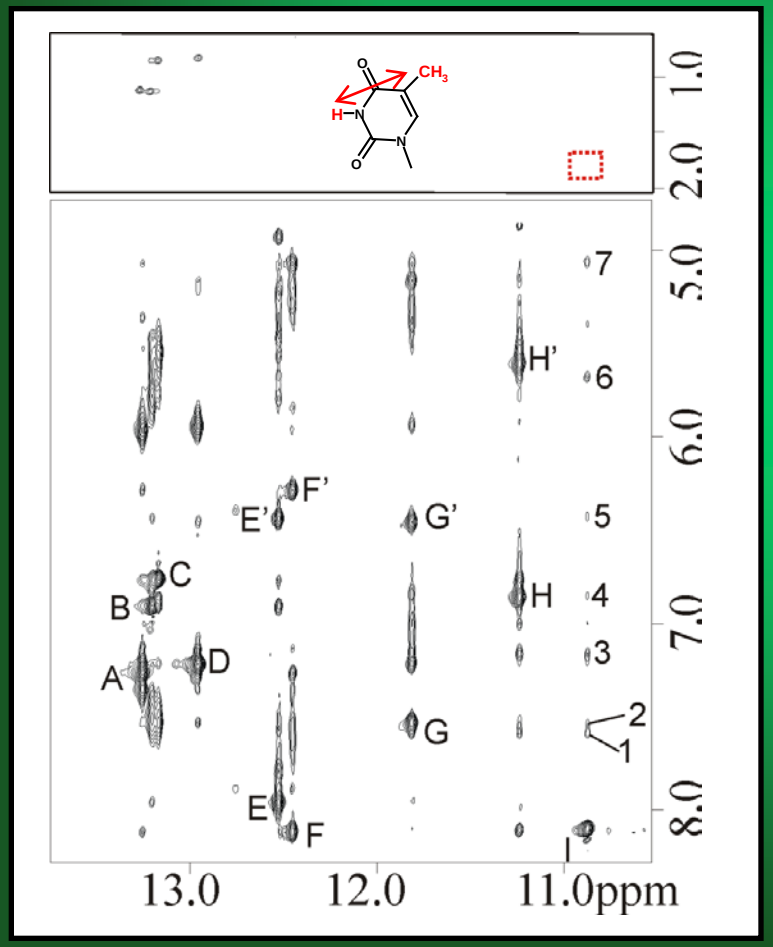

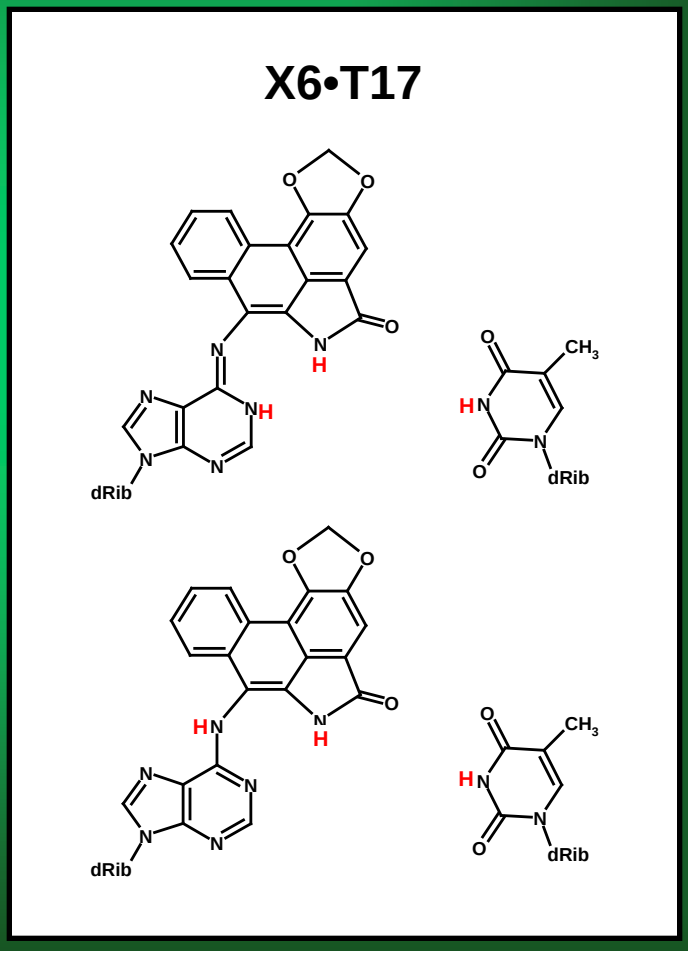

Lukin et al (2012) *Nucleic Acids Res.* 2012 40, 2759-2770.

dA-(N^6)-ALII Duplex

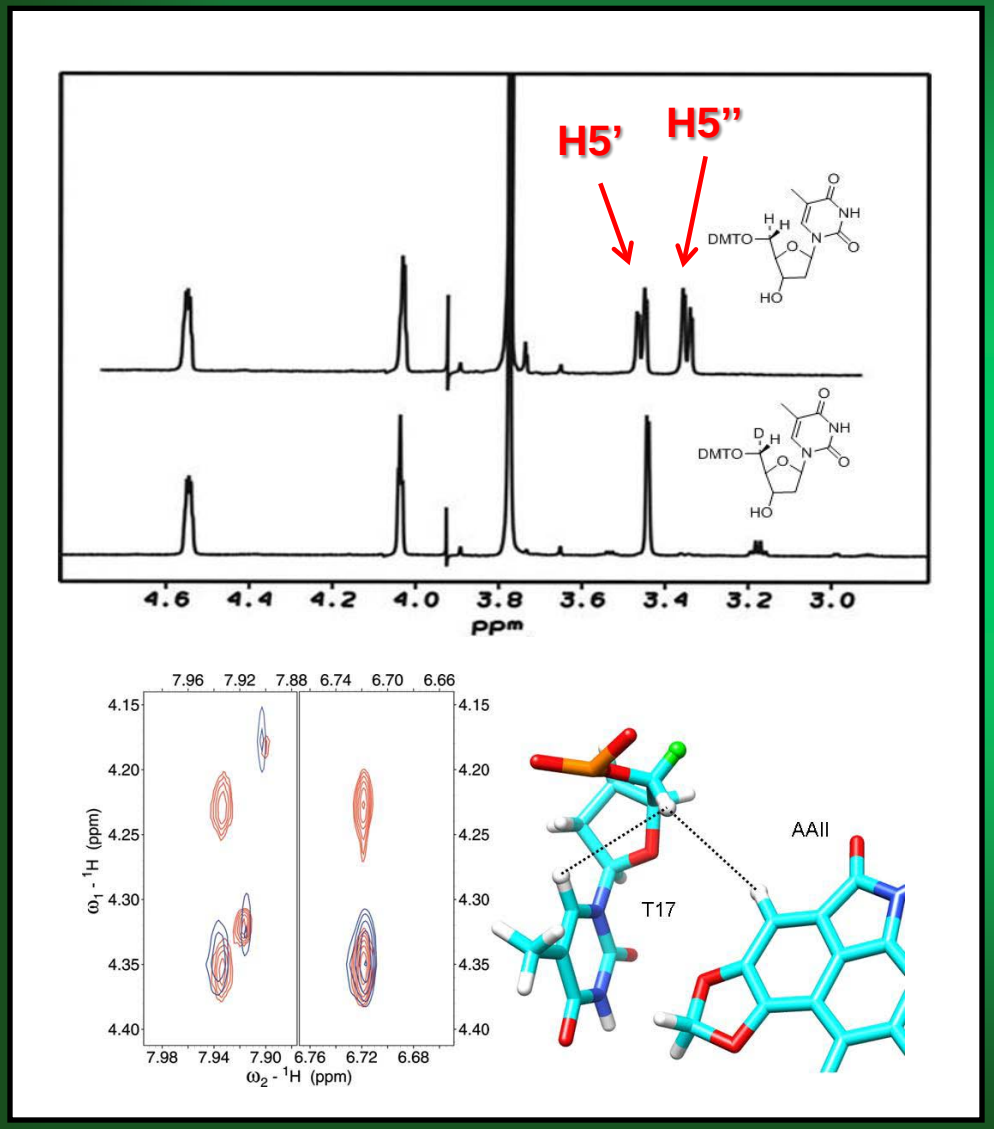

Selective H5"
thymine deuteration

Lukin & de los Santos (2010) *Nucleos. Nucleot. Nucleic Acids.*, **29**, 562-573.

dA-(*N*^{6})-ALII Duplex

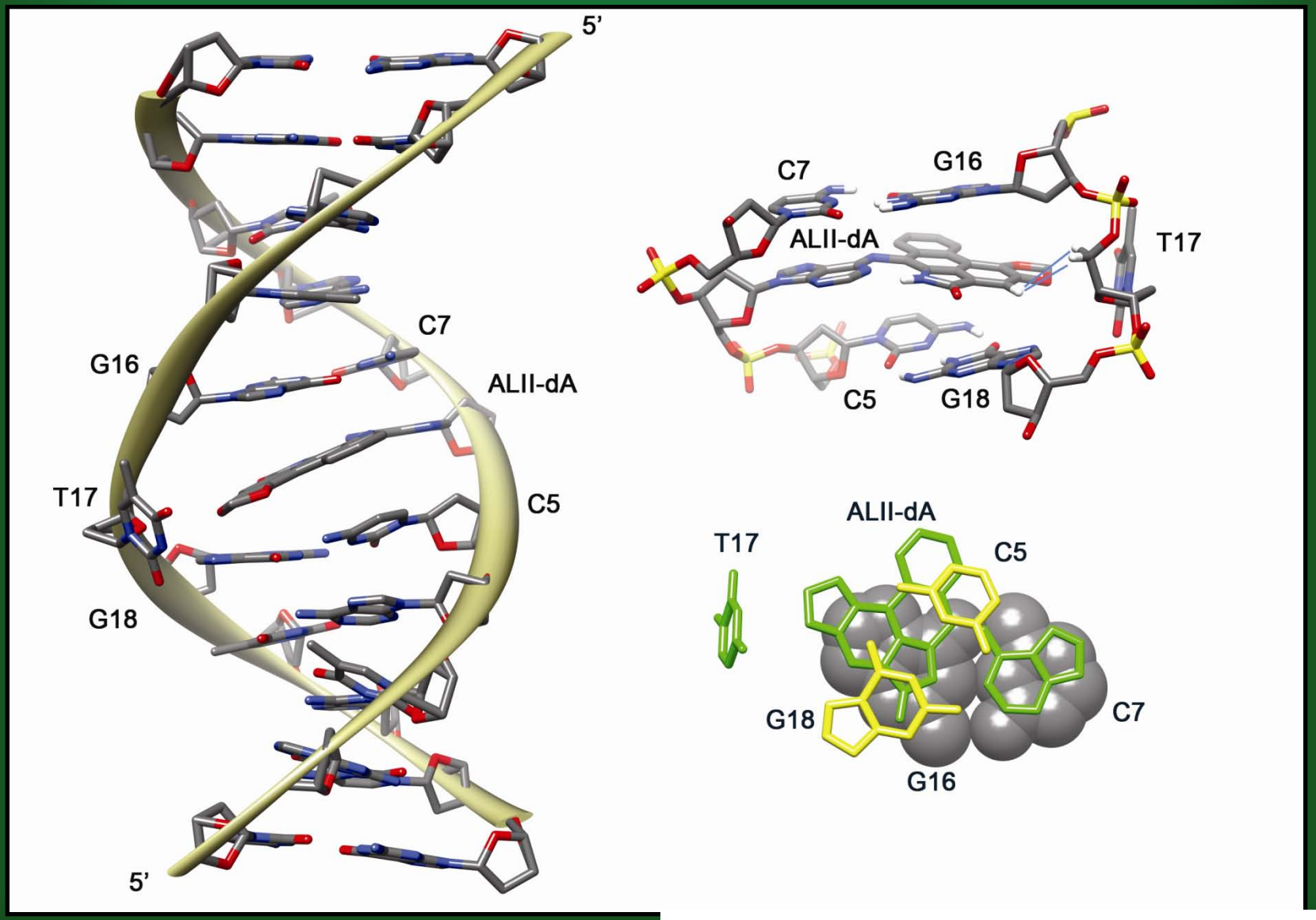

Lukin et al (2012) *Nucleic Acids Res.* 2012 40, 2759-2770.

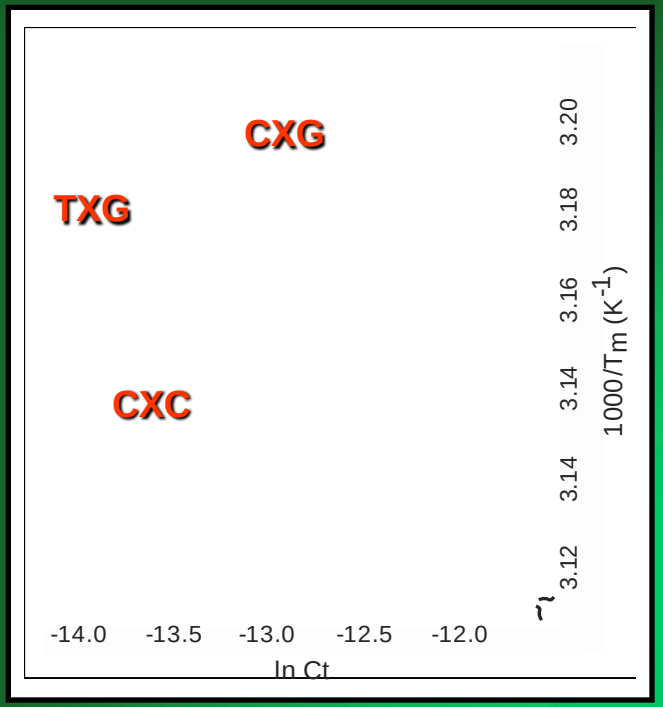

dA-(N^6)-ALII causes duplex destabilization

Duplex Sequence	T_m (°C)	ΔH^0 (Kcal/mol)	ΔS^0 (cal/mol °K)	$\Delta G^0_{25°C}$ (Kcal/mol)	$\Delta G^0_{37°C}$ (Kcal/mol)	$\Delta\Delta G^0_{37°C}$ (Kcal/mol)
C - X - C	45.2	-76	-211	-12.7	-10.2	2.5
C - A - C	51.6	-98	-273	-15.9	-12.7	
T - X - G	43.1	-58	-157	-11.2	-9.3	1.2
T - A - G	46.7	-78	-219	-13.1	-10.5	
C - X - G	39.9	-68	-190	-11.0	-8.7	0.8
C - A - G	42.9	-72	-203	-11.9	-9.5	

Lukin et al (2012) *Nucleic Acids Res.* 2012 40, 2759-2770.

The AL-II-dA lesion reduces the stability of the duplex

Duplex structure is perturbed at the lesion site. The AL-II moiety intercalates in the opposing strand displacing the partner thymine in the major groove

In spite of these changes, the duplex adopts a single conformation that is stabilized mainly by hydrophobic interactions at lesion site

Lukin et al (2012) *Nucleic Acids Res.* 2012 40, 2759-2770.

NER Recognition of Bulky Adducts

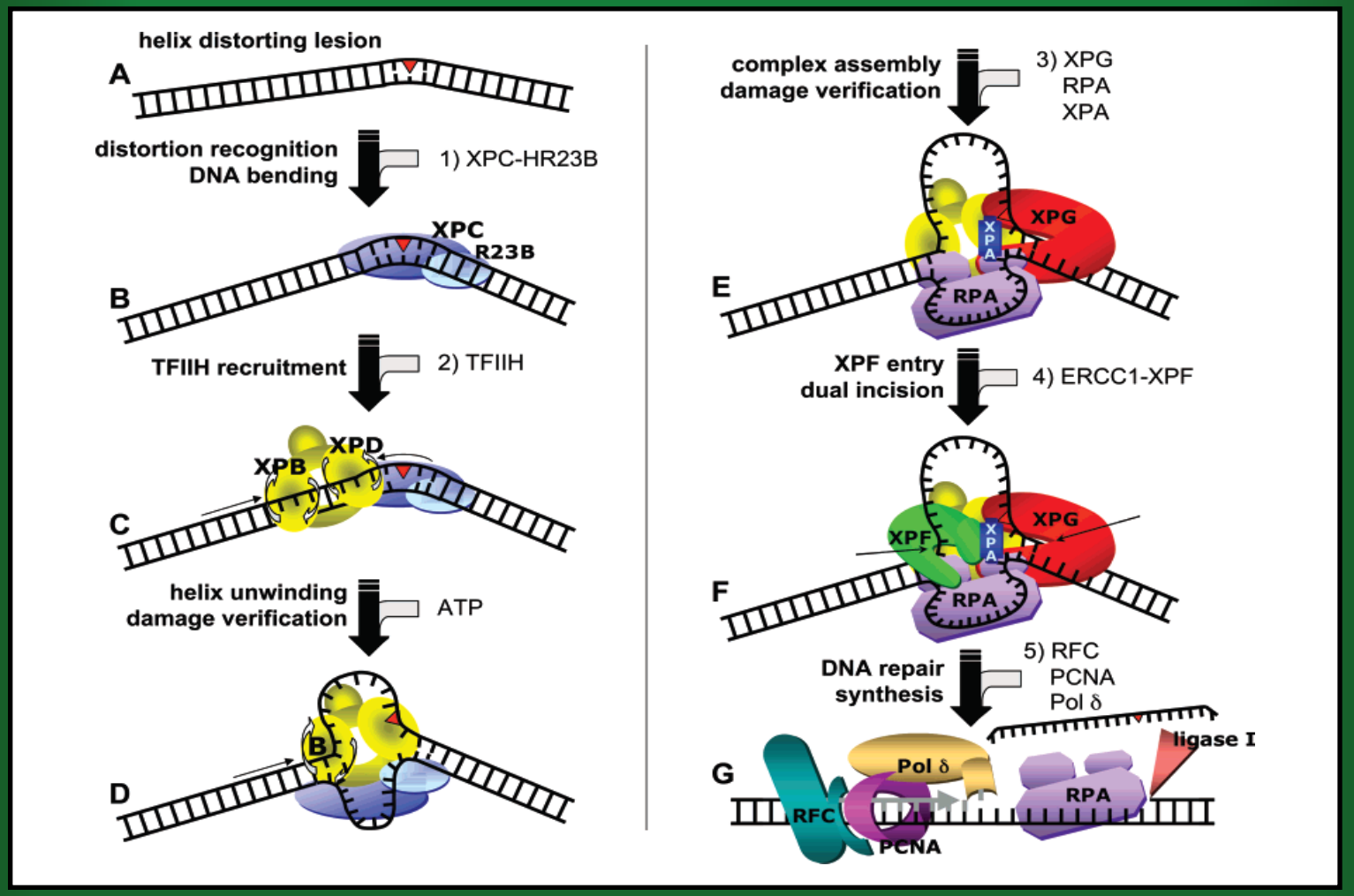

dA-(N^6)-AL-II adduct levels are elevated in GG-NER and transcription-coupled NER deficient cells, but not in XPC cell lines lacking GG-NER.

In vitro, plasmids containing a single dA-(N^6)-AL-II adduct are resistant to the early recognition and incision steps of NER.

Additionally, XPC-RAD23B, the GG-NER damage sensor, failed to specifically bind to dA-(N^6)-AL-II adducts.

Sidorenko *et al* (2012) Nucleic Acids Res. 40, 2494-2505

Recognition of bulky lesions by GG-NER seems less efficient than initially thought

Topology of duplex stabilizing lesions (AAF-*N*^{2}-dG, 3ABA-*N*^{2}-dG)

Stability threshold

Other factors